Reviewed Preprint
v1 • September 12, 2025
Not revised

Reviewed Preprint
v2 • April 30, 2026
Revised by authors

Distinct evolutionary trajectories of two integration centres, the central complex and mushroom bodies, across Heliconiini butterflies

Max S Farnworth[a] ✉, **Yi Peng Toh**[b], **Theodora Loupasaki**[a], **Elizabeth A Hodge**[a], **Basil el Jundi**[c,d], **Stephen H Montgomery**[a] ✉

[a]Evolution of Brains and Behaviour lab, School of Biological Sciences, University of Bristol, Bristol, United Kingdom • [b]Behaviour and Speciation, Faculty of Biology, Ludwig-Maximilians-Universität München, Munich, Germany • [c]Department of Biology, Norwegian University of Science and Technology, Trondheim, Norway • [d]Institute of Biology and Environmental Sciences, Carl von Ossietzky Universität Oldenburg, Oldenburg, Germany

For correspondence:
m.farnworth@bristol.ac.uk
s.montgomery@bristol.ac.uk

Competing interests: No competing interests declared

Funding: See page 29

Reviewing editor: Albert Cardona, University of Cambridge, United Kingdom

eLife Assessment

The analysis of neural morphology across Heliconiini butterfly species revealed brain area-specific changes associated with new foraging behaviours. While the volume of the centre for learning and memory, the mushroom bodies, was known to vary widely across species, these new, **valuable** results show conservation of the volume of a center for navigation, the central complex, but with specific changes in neuropeptide expression in the noduli and in the numbers of ellipsoid body ring neurons. The presented evidence is **convincing** for both volumetric conservation in the central complex and fine neuroanatomical differences associated with pollen feeding, delivered by experimental approaches that are applicable to other insect species. This work will be of interest to evolutionary biologists, entomologists, and neuroscientists.

https://doi.org/10.7554/eLife.107589.2.sa3

Abstract

Neural circuits have evolved to produce cognitive processes that facilitate a species' variable behavioural repertoire. Underlying this variation are evolutionary forces, such as selection, that operate on changes to circuitry against a background of constraints. The interplay between selection and potentially limiting constraints determine how circuits evolve. Understanding how this process operates requires an evolutionary framework that facilitates comparative analysis of neural traits, within a clear behavioural and functional context. We leverage a large radiation of Heliconiini butterflies to examine how selection shapes the evolution of the central complex and the mushroom bodies, two integration centres in the insect brain involved in spatial navigation. Within the Heliconiini, one genus, *Heliconius*, performs systematic spatial foraging and navigation to exploit specific plants as a source of pollen, a novel dietary resource. Closely related genera within Heliconiini lack this dietary adaptation, and are more vagrant foragers. The evolution of increased spatial fidelity in *Heliconius* has led to changes in brain morphology, and in specific learning and memory profiles, over a relatively short evolutionary time scale. Here, using a dataset of 41 species, we show that in contrast to a massive expansion of the mushroom bodies, the central complex and associated visual processing areas are strongly conserved in size and general architecture. We corroborate this by characterising patterns of fine anatomical conservation, including conserved patterns in dopamine and serotonin expression. However, we also identify a divergence in the expression of a neuropeptide, Allatostatin A, in the noduli, and in the numbers of GABA-ergic ellipsoid body ring neurons and their branching in the fan-shaped

body, which are essential members of the anterior compass pathway. These differences match expectations of where evolutionary adaptability might occur inside the central complex network and provide rare examples of divergence of these circuits in a shallow phylogenetic context. We conclude that due to the contrasting volumetric conservation of the central complex and the massive volumetric differences in the mushroom bodies, their circuit logics must determine distinct responses to selection associated with divergent foraging behaviours.

Introduction

Intricate patterns of interconnecting neurons in the brain are the anatomical basis of the processes that facilitate behaviour, be it an innate response to specific sensory cues or the integration of external cues with internal information [1,2]. As evolutionary processes act on variation in behavioural traits and responses, local circuits must alter behaviour in the context of selection acting on the output of the larger system [3]. These alterations also occur in the context of a system's ability to respond to change (adaptability) which is in turn shaped by a range of potential constraining factors, be it to maintain ancestral or interrelated functions, or through partially shared deterministic developmental programs [4–6].

A collection of neural circuits particularly suited to examine the interplay of constraints and adaptability are those that support experience-dependent spatial foraging behaviours in insects. Here, two well-studied brain regions, the mushroom bodies and the central complex, integrate multiple cues used for foraging such as visual landmarks, odour plumes as well as other directional cues to guide navigational behaviours [7–11]. The mushroom bodies, often referred to as the learning and memory centres of the insect brain, integrate multimodal sensory information with past experiences to modify a multitude of downstream connections according to learned and memorized contexts [12,13]. Similarly, the central complex, known as the navigation centre of the insect brain, relies on multisensory information [14–16] to produce steering signals by comparing the insect's current heading direction with its goal direction [17–20]. The central complex receives input from the mushroom bodies in a subregion, called the fan-shaped body, via mushroom body output neurons (MBONs) [21]. This likely allows insects to flexibly modify their navigational goal based on internal preferences, experience-related olfactory and visual cues, and behavioural context [22,23]. Such behavioural flexibility is of high importance during spatial foraging where the same location is repeatedly visited over time to exploit a reliable resource, while incorporating behavioural responses to new opportunities, or threats [24,25].

Interestingly, while the mushroom bodies repeatedly show patterns of adaptability through volumetric expansion and internal structural change across insects [26–30], the size and general morphology of the central complex appears to be more conserved, potentially reflecting evolutionary constraints (Figure 1A-B) [31]. For example, an elaboration of spatial foraging and associated long-term memory is concomitant with an expansion of their mushroom bodies in some lepidopterans, as well as in Hymenoptera [27,29,30,32], but changes in the central complex associated with spatially faithful foraging are less well characterised, and apparently less prominent [33]. However, their mutual functions in spatial foraging behaviour predict that adaptive changes in one of these neural circuits could have the potential to influence the structure and function of the other, resulting in a pattern of coevolution. As such, the contrasting degrees of interspecific variation and functional interdependence provides an intriguing basis to make inroads into the evolutionary dynamics underlying neural circuit changes across the anatomical boundaries of brain components.

Here, we provide a closer examination of whether changes in mushroom body architecture co-occur with altered central complex investment or structure. We leverage a closely related tribe of Neotropical butterflies, the Heliconiini, as a model system. Within Heliconiini, the genus *Heliconius*, exhibits a pattern of spatially faithful foraging behaviour, consistent with trap-lining, to efficiently forage pollen from spatially distributed, but temporally reliable, floral resources [32,34–37]. To form spatially faithful foraging routes, cues associated with these sites need to be recalled based on time-stable, long-term memory of spatial locations [38–40]. This complex foraging behaviour is likely supported by changes in the circuits involved in learning, memory, and spatial

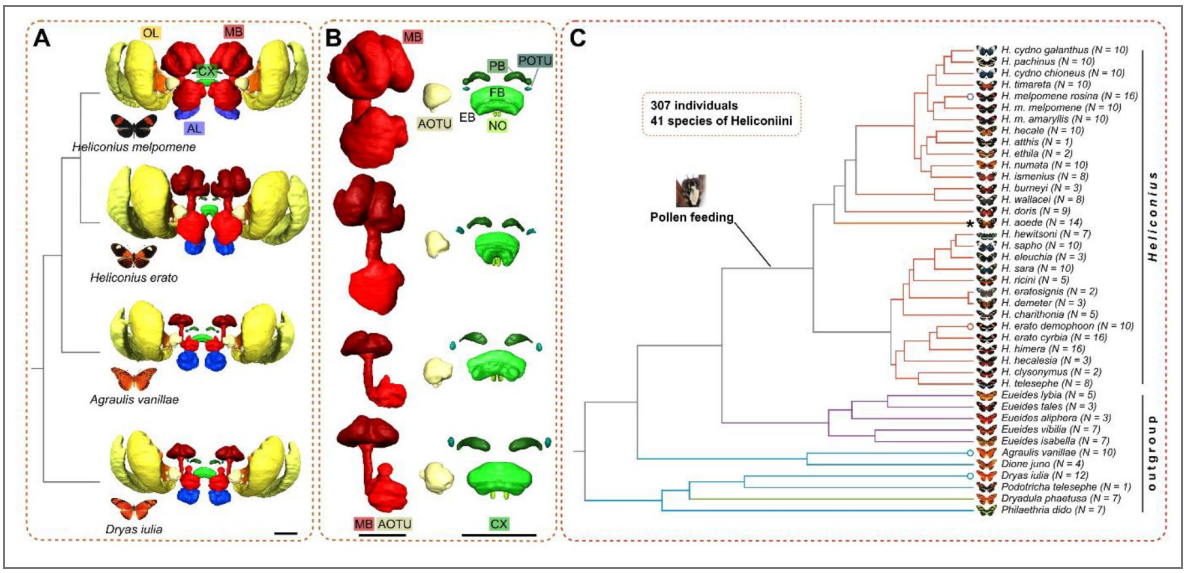

Figure 1. Introduction to the Heliconiini system used in this study.

A: The Heliconiini feature a previously reported expansion of the mushroom bodies in *Heliconius sp*. concomitant with a dietary innovation of pollen feeding. Shown are 3D segmentations of the OL, AL, MB, CX, AOTU and POTU in the brain of four exemplary species. **B**: Examining the CX of these four species already indicates that CX volume seems conserved, relative to variation in the MB. Shown are separate 3D segmentations of the MB and AOTU as well as the CX and POTU, with the CX and POTU consistently enlarged (i.e. not to scale to the MB models). **C**: To assess divergence in volumetric investment in these structures we used a dataset of 307 individuals of 41 species of Heliconiini. Depicted is the phylogeny [109] with species names, appearance and number of individuals per species. Species shown in A and B are indicated here by a circle at the end of each edge. Colour indicates focal groups here and elsewhere [29]. The asterisk at the branch of *H. aoede* indicates a secondary loss of pollen feeding. Scale bars are always 250 µm. Abbreviations: OL optic lobe, AL antennal lobe, MB mushroom bodies, CX central complex, AOTU anterior optic tubercle, POTU posterior optic tubercle, PB protocerebral bridge, FB fan-shaped body, EB ellipsoid body, NO noduli.

navigation, with *Heliconius* exhibiting the capacity to learn spatial information at large distances [41], likely using landscape features [35], and an enhanced capacity for learning complex visual cues [29] and to retain visual memories for prolonged periods of time [36,37]. Interestingly, other genera within the Heliconiini share life history traits, habitats and wider ecologies with species of *Heliconius* [42,43]. However, they do not use pollen as a food source, and are not known to form long-term stable home ranges or perform the derived foraging strategies of pollen feeding *Heliconius* [32]. This increased reliance on spatial memory for faithful patterns of foraging in *Heliconius* suggests that divergent selection pressures between *Heliconius* and their closest relatives will have acted on the navigation circuits of the brain. Indeed, this stark behavioural divergence of a pollen feeding innovation coincided with a massive expansion of mushroom body volume, and structural changes in both the input sites, reflecting specialisation toward visual processing, and the output sites, reflecting possible specialisations in specific memory types [28,29,36]. These adaptations in the mushroom body occur without apparent changes in upstream sensory pathways [29,44], but the effects on downstream circuits have not been examined yet. The relatively shallow phylogenetic distances across Heliconiini, and their similarity in most behavioural domains provide a unique context in which to disentangle the effects of mushroom body expansion on interacting circuitries, including the central complex. Indeed, these circumstances permit us to test the hypotheses that modifications in the mushroom bodies either occurred in isolation from other integrative centres, or that they occurred in concert with specific changes in centres, such as the central complex. This provides insights into the functional flexibility of two interacting, integrative centres across evolutionary time.

To understand how the cognitive demands of pollen feeding and systematic foraging shaped the evolution of the central complex in *Heliconius*, volumetrically as partner of the mushroom bodies, but also in terms of its finer anatomy, we combined phylogenetically broad sampling of neuropil volume with fine anatomical descriptions among representatives of key lineages. To assess evidence of volumetric changes in the central complex and associated neuropils, we drew data from a large dataset of immunostained brains from 307 individuals of 41 species, to determine patterns of evolution using phylogenetic modelling. We then used a series of stainings, primarily targeting classic neurotransmitters, to examine fine anatomical patterns beyond volumetric effects in a targeted group of species and individuals. The combination of phylogenetically deep data and fine-anatomical approaches in select species allowed us to examine patterns of mushroom body and central complex co-evolution in the adaptation to a novel food source.

Results

We examined the evolution of central complex (CX), anterior optic tubercle (AOTU) and posterior optic tubercle (POTU) investment, in the context of the previously characterized expansion of the mushroom bodies (MBs) across Heliconiini. We used a combination of phylogenetic comparative analysis across a large dataset of brains immunostained against the structural marker synapsin in 41 species and 307 individuals, and more targeted sampling of species that represent the behavioural and neuroanatomical diversity of Heliconiini for more fine-scale assessments of patterns of divergence in substructures of the CX with various antibodies (Figure 1A-B). In doing so we provide the first comparative assessment of the CX in this emerging case study in neural evolution. The CX spans the midline and consists of four neuropils, the protocerebral bridge (PB), the noduli (NO) as well as the fan-shaped body (FB) and ellipsoid body (EB) which together constitute the central body (CB) (Figure 1B). The AOTU is localised antero-lateral to the CX and is a key processing centre of the insect compass pathway of the central brain, transmitting information from the AOTU via tubercular-bulbar (TuBu) neurons to the bulb (BU) where ellipsoid body ring (ER) neurons then transfer the information to columnar neurons of the CX [45–47] (Figure 1B). The POTU is an optic glomerulus of the central brain that lies postero-lateral to the protocerebral bridge, close to the posterior optic commissure. The POTU receives synaptic input from the accessory medulla of the optic lobe and forms tight connections with the protocerebral bridge through polarisation-sensitive neurons in some insect species [48–50]. Both the AOTU and POTU are easily discernible neuropils and form clear connections with different parts of the CX, allowing us to test for effects of circuit change in tightly connected sister circuits beyond the CX.

Isolated impact of mushroom body expansion within the central complex, AOTU and POTU circuit

To assess whether cognitive traits associated with pollen feeding not only evolved concurrently with expansions of the mushroom bodies (MB) [29] but also with volumetric changes in the CX and its closely associated visually linked neuropils, the AOTU and POTU, we determined volumes of all CX neuropils (PB, FB, EB and NO), as well as the combined volume of the three subunits of the AOTU, and the POTU, in our phylogenetic dataset of 41 species of Heliconiini butterflies (Figure 1C).

We first examined the effects of mushroom body expansion on CX evolution by testing the relationships between the presence of pollen feeding (PF), clade membership (defined as groups with distinct degrees of expansion, identified previously [29]) and mushroom body size (*MB * PF*; *MB * Clade*) on the volumes of the CX, its constituent neuropils as well as the AOTU and POTU (Table 1 for model overview). Throughout the CX, AOTU and POTU, as well as within the CX neuropils, no significant changes in volumetric investment were detected that were associated with pollen feeding, clade membership, and mushroom body size (Figure 2A-B, Figure S2, Table 1). We observed a very tight association with our allometric control (central brain size minus focal neuropils; rCBR). We did identify significant associations between MB size on CX size (Indications in Figure 2A-B), isolated from the presence of pollen feeding or clade membership. However, this reflects the remaining effects of allometric scaling between brain components, rather than non-allometric shifts reflecting the effects of divergent selection.

We next wanted to corroborate the distinct absence of volumetric expansions in the CX, coincident with mushroom body expansion or otherwise, by examining evolutionary rates of change in CX, AOTU and POTU volumes in comparison with rates of MB expansion [29]. Previously, Couto et al [29] identified very high evolutionary rates of mushroom body expansion at the base of *Heliconius* where pollen feeding evolved. In contrast, we found a distinct absence of any changes in the evolutionary rate of CX size (Figure 2 C/D, Figure S3A). Analogous analyses for the AOTU and POTU revealed similar levels of consistent, low rates of evolution during key evolutionary periods of ecological transition (Figure S3B-C). Minor evolutionary rate changes were observed in select terminal branches (e.g. for the CX in *Heliconius burneyi, hecale* or *Eueides aliphera;* Figure 2D,

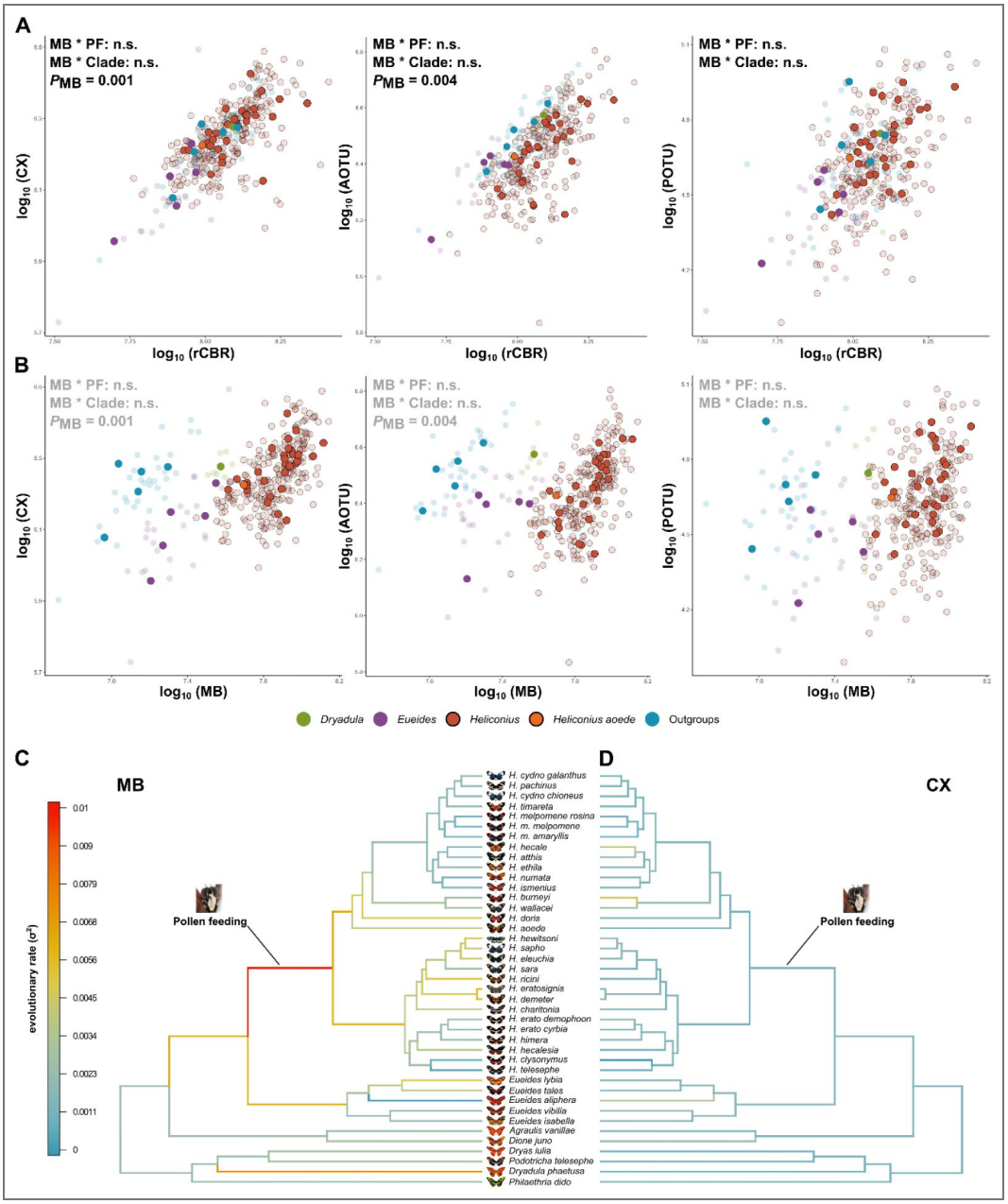

Figure 2. The central complex, the AOTU and POTU do not show pollen-feeding linked patterns of volumetric expansion or increased evolutionary rates.

A/B: Assessments of the effects of mushroom body size interacting with pollen feeding and with previously identified expansion events in the sum of all CX neuropils (total CX), AOTU and POTU, and in separate CX neuropils (see Figure S2). Shown are each neuropil against a measure of whole brain size, rCBR (A), as well as against MB size (B). Results are indicated in each panel; first, the effects of each interaction by assessment of DIC differences, and then the significance of the relationship between the MB and each neuropil. Colour coding was done according to clade differences in mushroom body size identified previously [29]. Solid data points indicate species averages, while opaque circles indicate individual data points. Black contours indicate *Heliconius sp*. data points. **C/D**: Analyses of evolutionary rates of MB size relative to rCBR (**C**), and CX size relative to rCBR (**D**), which reveals two very distinct evolutionary patterns. In the MB (**C**) particularly high rates of evolution have previously been identified on the branch leading to *Heliconius* [29], coincident with the innovation of pollen feeding. At the same branching point we see relatively low rates of evolution in CX size (**D**). Both phylogenies are shown at the same scale (see Figure S3 for a CX tree with absolute scale of evolutionary rates). The pollen feeding photograph is kindly provided by Sebastian Mena. CX central complex, AOTU anterior optic tubercle, POTU posterior optic tubercle, MB mushroom bodies, rCBR rest of the central brain. PF pollen feeding.

S3A) but are not associated with known behavioural changes or MB expansion (Figure 2C). We therefore conclude that the neural changes accommodating cognitive demands for pollen feeding did not include volumetric expansion and or increased investment in the CX (and its neuropils), or in the wider visual pathway that feeds into the CX (AOTU and POTU). The CX therefore evolves as a distinct system compared to the major volumetric expansion in the MB.

Mosaic patterns of co-dependency between central complex neuropils, AOTU and POTU

We next explored how the different CX neuropil and AOTU/POTU volumes co-vary with each other, and to what extent these interspecific scaling relationships of volumes mirrored known functional links between neuropils. Moreover, we tested whether these co-evolutionary relationships were altered during mushroom body expansion.

We first examined whether variation in each structure is determined by variation in all other structures using multiple regression analyses. This revealed a mosaic pattern of co-variation, where the AOTU positively scaled with FB and EB, the POTU with PB, the FB with EB and the EB with the PB, but all other structural pairings scaled independently of each other (Figure 3A). To determine whether any of these dependencies were impacted by the origin of pollen feeding we re-ran the significant pair-wise regressions including presence of pollen feeding as a factor. This revealed that all scaling relationships were robust to the presence or absence of pollen feeding, indicating conserved co-evolutionary relationships across the tribe.

Indeed, we found that the presence of dependencies can illustrate, in most cases, anatomical and functional links that may mutually constrain variation in these structures through characteristic cell types (Figure 3B and C), whose nomenclature derives from the neuropils they connect. The most relevant for the scaling relationships we observed are the EPG (connecting the **E**B, **P**B, and part of the lateral complex, the **G**all), PFN (PB-FB-NO), PEN (PB-EB-NO), PFL (PB-FB-LAL), ER (BU-EB) and Δ7 (POTU-PB) neurons [21,45,46,51–55] (Figure 3B). The majority of results from pairwise scaling comparisons match what we would expect from these known cell types and prominent connectivity patterns, but some do not. Although these results require further investigation, we interpret our results as evidence that some of the within-scaling co-evolutionary relationships of the CX may be determined by functional co-dependence, but that the evolution of pollen feeding and mushroom body expansion has not altered these internal relationships. This would be consistent with a largely conserved circuit architecture.

Conserved tract and synaptic architecture in the Heliconiini central complex

We next sought to test our interpretation more closely by assessing whether other factors beyond size are obscured by the conserved volume of the CX. We first examined the CX with general labels to examine the complete CX architecture of a representative outgroup, *Dryas iulia*, and a pollen feeding *Heliconius*, *Heliconius erato* (Figure 4). We then used several antibodies targeting neurotransmitters and neuropeptides, as well as bulk injections of portions of cell populations labelled, to more closely examine the anatomy of the CX (Figures 5, 6 and S4), and to identify anatomical divergences in selected markers (Figures 7, 8 and S5).

We first used general antibodies targeting acetylated tubulin to visualize neuronal tract anatomy, and horseradish peroxidase (HRP) to determine synaptic areas [56]. Not surprisingly, these general labels revealed a very conserved architecture and a stereotypical makeup of the CX, very comparable to the Monarch butterfly CX (Figure 4A/B) [57], briefly summarised as:

A. **Noduli**: We tentatively defined four layers of the noduli (Figure 4C/D). However, the exact boundaries were difficult to determine without additional markers as any tracts, which often can be used as suitable landmarks for compartment borders [58], were too small inside the noduli. We also note a general variability in left and right-side symmetry of the noduli. In part, this matches previous observations into nodulus anatomical variation [55].
B.

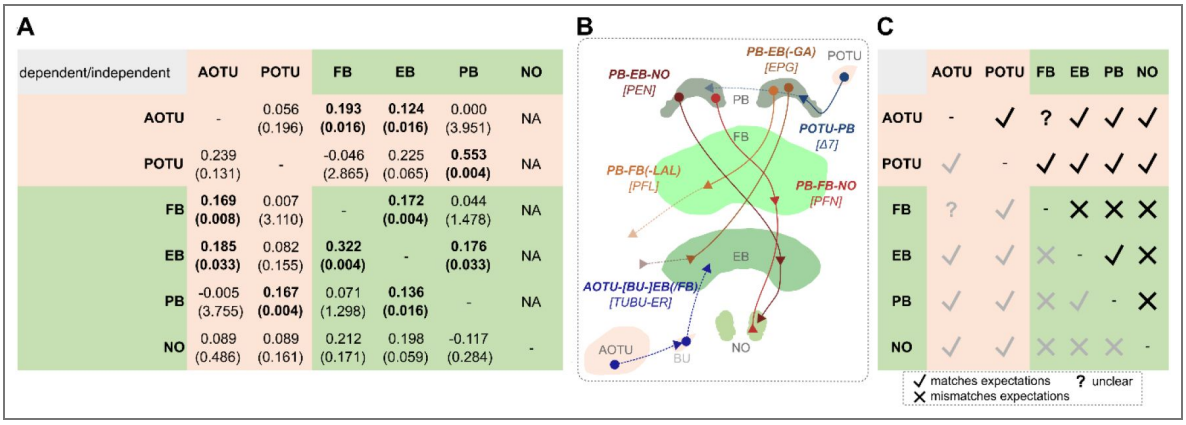

dependent/independent	AOTU	POTU	FB	EB	PB	NO
AOTU	-	0.056 (0.196)	**0.193 (0.016)**	**0.124 (0.016)**	0.000 (3.951)	NA
POTU	0.239 (0.131)	-	-0.046 (2.865)	0.225 (0.065)	**0.553 (0.004)**	NA
FB	**0.169 (0.008)**	0.007 (3.110)	-	**0.172 (0.004)**	0.044 (1.478)	NA
EB	**0.185 (0.033)**	0.082 (0.155)	**0.322 (0.004)**	-	**0.176 (0.033)**	NA
PB	-0.005 (3.755)	**0.167 (0.004)**	0.071 (1.298)	**0.136 (0.016)**	-	NA
NO	0.089 (0.486)	0.089 (0.161)	0.212 (0.171)	0.198 (0.059)	-0.117 (0.284)	-

Figure 3. Central complex neuropils and associated areas show different patterns of scaling with each other.

A: Tests of significant scaling relationships between each substructure on the left, as dependent variable, and all others as independent variables. Each cell indicates the test statistic (posterior mean) and the *P* value in parentheses, and if significant is shown in bold. As values for NO were only available for parts of the total dataset, noduli were not included as independent variables. **B**: Prominent cell types that interconnect central complex neuropils and the AOTU and POTU, which may potentially explain patterns of neuropil scaling, if positive scaling relationships indicate co-evolution among functionally interdependent structures. Cell type depictions are examples with localisation inside each neuropil being purely visual (as well as their colour), while triangles indicate approximate output sites. Namings first refer to the connected neuropils, then in brackets to established nomenclature, based on current literature [21,45,46,51–55]. **C**: A depiction of where our data showing significant scaling relationships (A) matches (check mark), or mismatches (X), expectations that are based on prominent (mostly columnar) neuron classes and connections (B). Where expectations are unclear, we have annotated the comparison with (?). Specifically, we would normally not expect positive scaling between AOTU and FB, but this may be explained by findings in Figure 7 and an increased population of ER neurons projecting to the FB. Generally, this diverse pattern indicates that more variation occurs throughout the system than can be captured in this volumes-based analysis. AOTU anterior optic tubercle, POTU posterior optic tubercle, PB protocerebral bridge, FB fan-shaped body, EB ellipsoid body, NO noduli, GA gall.

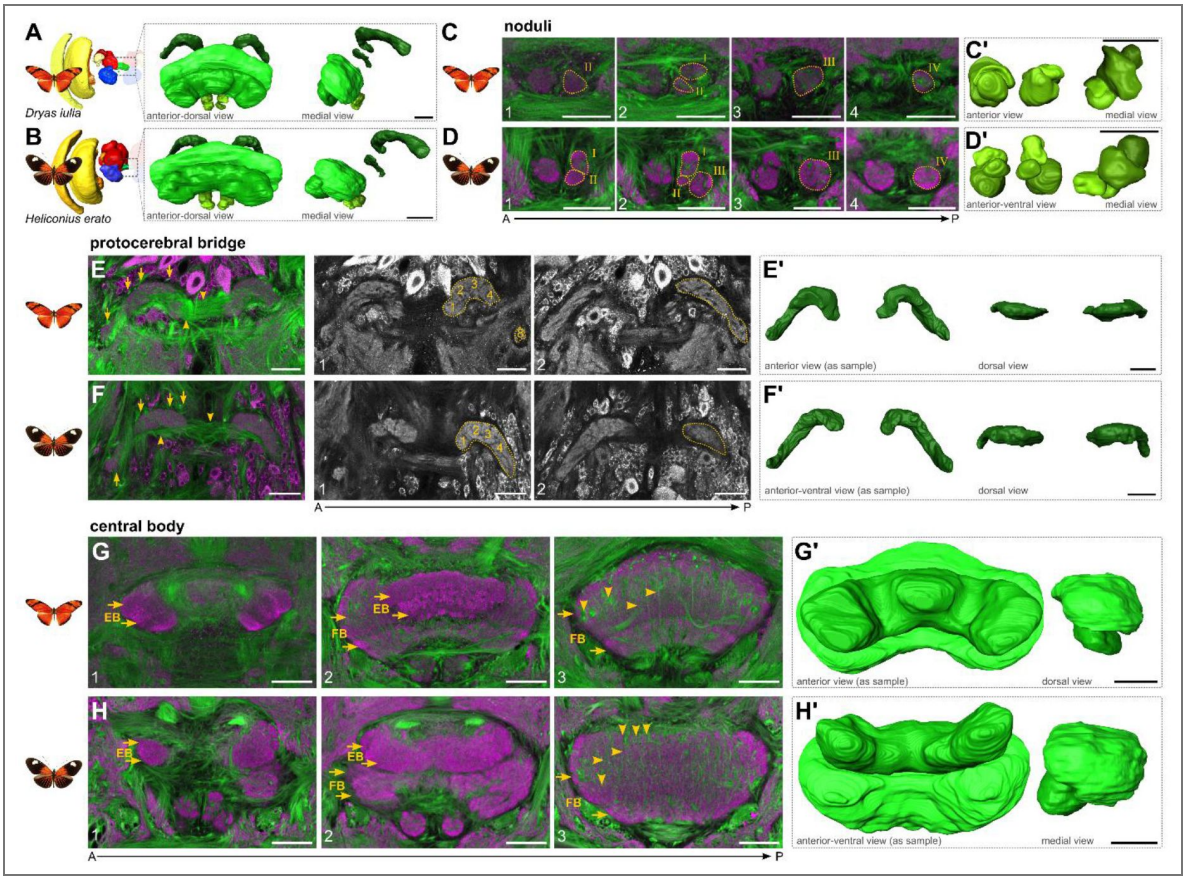

Figure 4. Tract and synaptic labelling reveal a conserved central complex architecture in Heliconiini butterflies.

A/B: Double labelling of tubulin (green) and HRP (magenta) was used to reveal the synapse-dense areas of the central complex as well as its underlying tract systems. **C/D**: Noduli architecture reveals, tentatively, a conserved pattern of four main domains, but with very pronounced asymmetry between hemispheres. **E/F**: Tract bundles close to the PB associate with DM1-4/WXYZ tracts (arrows). Tangential neuron bundles project across hemispheres through the PB (arrowheads). HRP alone (grey) allows a rough approximation of vertical columns in the PB (a-h). **G/H**: Labelling reveals two distinguishable layers in the fan-shaped body while additional staining elsewhere reveals further detail (arrows in G/H-2/3). Thicker tract conflations indicate the columnar architecture determined through the four columnar neuron bundles (arrowheads in G/H-3). Labelling in the EB reveals two pronounced layers (arrows in G/H-1/2), while obvious columns could not be indicated. PB protocerebral bridge, FB fan-shaped body, EB ellipsoid body. A anterior, P posterior. Scale bars are 50 µm. See animated 3D segmentations and annotated stacks in file repository.

Protocerebral bridge: The protocerebral bridge was generally conserved (Figure 4E/F). Like in other lepidopteran species [57], the protocerebral bridge is split into two halves that are connected across the brain hemisphere via a commissural tract. Tubulin allowed us to determine tract conflations that form the WXYZ tracts (also known as DM1-4 tracts) that interconnect the protocerebral bridge with the central body via columnar neurons (arrows in Figure 4E/F) [59]. We labelled a tentative columnar array of eight columns of the protocerebral bridge in each hemisphere (Figure 4E/F-1).

C. **Fan-shaped body**: In the fan-shaped body, we were able to distinguish a dorsal and a ventral layer based on the tubulin and HRP stainings. Note that, with subsequent neurotransmitter stainings and mass injections, we were able to further subdivide the fan-shaped body into a total of four layers (arrows in Figure 4G/H-2/3 and Figure 5 & 6). Tracts enter the synapse-dense neuropil in very stereotypical fashion, indicative of the tracts that correspond to the columnar neurons of the DM1-4 lineages, which give rise to the columnar architecture of the fan-shaped body (arrowheads in Figure 4G/H-3).

D. **Ellipsoid body**: In the ellipsoid body, we also observed two prominent layers through HRP staining (Figure 4G/H-1/2), but using subsequent stainings identified four layers (Figure 6). Note that the 3D segmentations in Figure 4G' and H' might suggest different shapes of the ellipsoid body, but this is rather due to slightly different positioning of the brain relative to the axis of imaging.

The layering of the fan-shaped body and its columnar architecture indicated by tubulin and HRP combinations was corroborated by mass injections of Dextran into the superior medial and lateral protocerebrum (SMP, SLP) of *Dryas iulia*, which revealed a distinct labelling of fan-shaped body layers I, II and IV (Figure 5A), originating from dorsal as well as ventral projections (Figure 5B-D). With these injections we were able to determine fan-shaped body columns in layer IV particularly, and four tract conflations of the dorsal projections (arrowheads in Figure 5B), originating from the superior medial protocerebrum (Figure 5C). Some of the ventral projections seemed to directly originate from the γ lobe, a portion of the mushroom body, thus potentially labelling projections of mushroom body output neurons into the fan-shaped body (Figure 5a-c) [12,21].

Overall, the injections, standard labels and neuromodulatory stainings revealed two major groups of input channels consistently across species. A ventral projection that enters from ventrolaterally, in most cases into the central body (Figure 5D, Figure 6A-F), and one that originates from the superior lateral or medial protocerebrum, often with its dendritic fields unclear, and projects dorso-laterally or medially into the central body (Figure 5B-C, Figure 6A-F). These seem to be part of conserved supply channels, as they are also observed in *Drosophila* connectome data and data of the hemimetabolous *Schistocerca sp*. (see Figures 5, 6 and 8 in [45] and information in [51]) with recognizable projection patterns, despite strong shape differences.

Conserved patterns of serotonergic and dopaminergic neurotransmitter expression in central body layers

To more closely assess fine anatomical details of the Heliconiini CX and identify potential species differences, we performed neurotransmitter (GABA, Dopamine, Serotonin; Figure 6, 7 and S4), neuropeptide (Allatostatin A, Figure 8) and cell adhesion molecule (Fasciclin-II) stainings (Figure 6). This group of stainings served three overlapping purposes. First, to reveal closer details of general anatomy of the Heliconiini CX, with particular emphasis on central body layering, which proved more difficult with general markers (Figure 4, 6C/F/I/L). Second, to examine differences in the expression of important neurotransmitters. And third, through more sparse labelling, to identify any anatomical and structural differences that might be obscured by volume as well as general markers.

We first identified conserved patterns in dopaminergic and serotonergic neurons as well as in neurons labelled by Fasciclin-II (Figure 6). To label dopaminergic neurons, we used a Tyrosine Hydroxylase (TH) antibody, which resulted in much less prominent staining inside the CX itself (Figure 6A-C). However, through dorsal projections above the fan-shaped body, we could detect

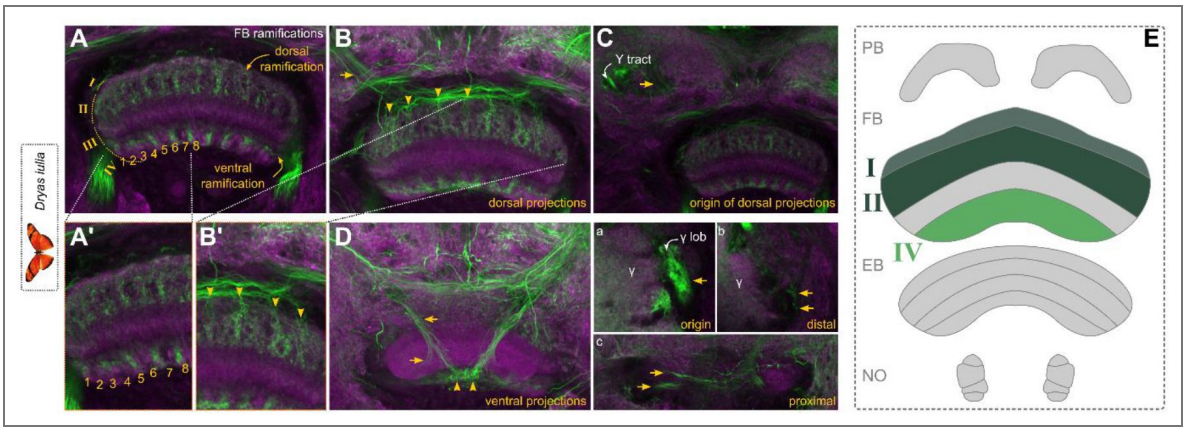

Figure 5. Mass injections in *Dryas iulia* reveal columnar architecture and input into the fan-shaped body.

A: A single injection into the superior median and lateral protocerebrum (SMP/SLP) of *Dryas iulia* has revealed prominent labelling of the fan-shaped body, particularly layers I, II (dorsal projection) and IV (ventral projection). **B:** Input pathways into these layers from a dorsal set of projections through four input tracts into the fan-shaped body (arrowheads), originating from the SMP/SLP region (**C**, arrow), whereas A' and B' are close-ups of A and B, highlighting the unique columnar architecture of the fan-shaped body revealed through this labelling. **D:** Ventral projections also seem to originate from the SMP/SLP region but are hard to trace. **a-c** depict close-ups of an interesting input pathway from γ lobe and lobelet into the fan-shaped body through the ventral projection. **E:** Schematic of labelling in generic central complex. Abbreviations: FB fan-shaped body, lob lobelet of the mushroom body. Scale bars equal 100 μm.

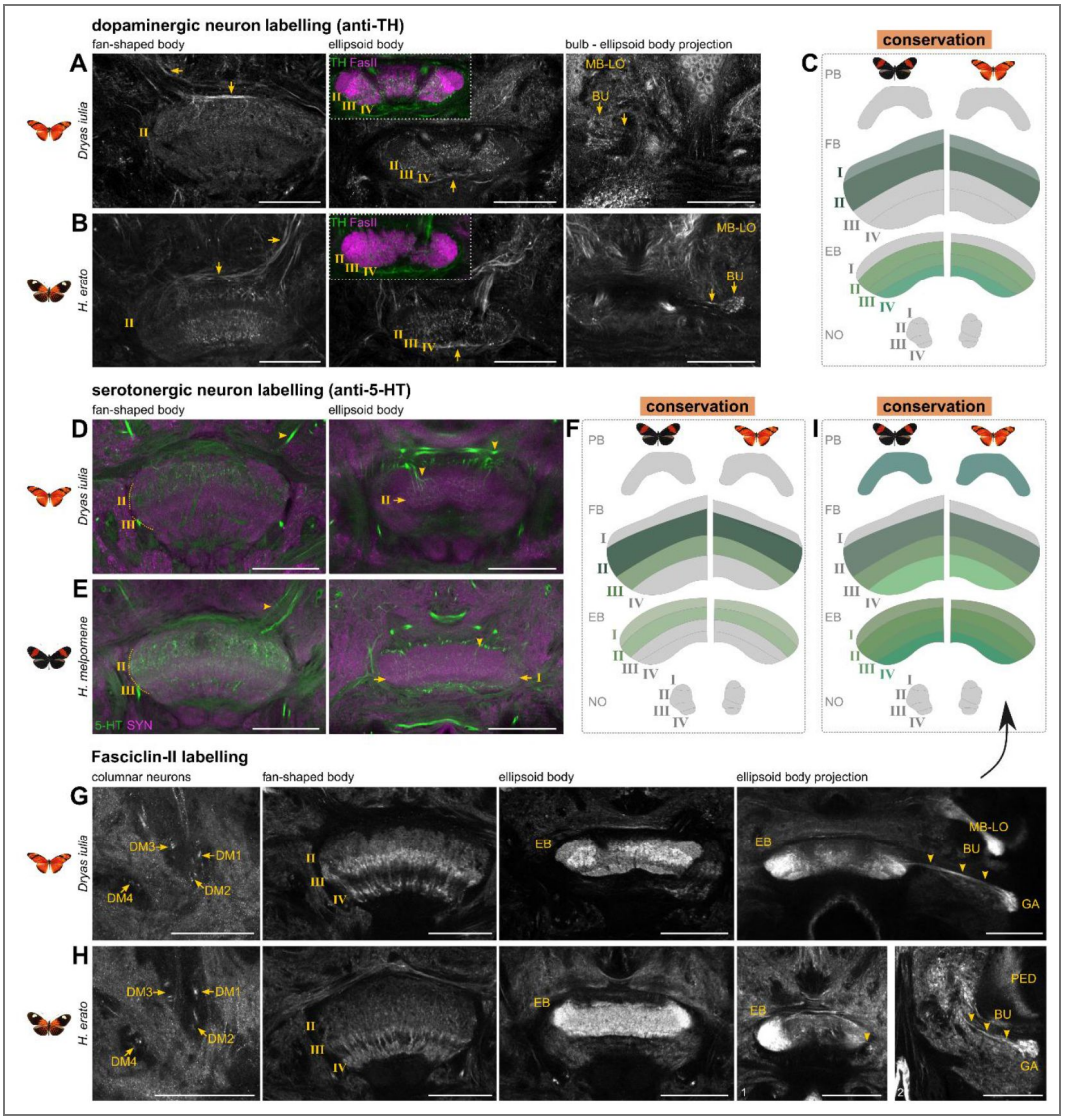

Figure 6. Comparative anatomical analysis of the Heliconiini central complex examining dopaminergic and serotonergic neurons and Fasciclin-II expression supports a largely conserved neurotransmitter expression and anatomy.

Shown are original data and a schematic of the central complex summarising expression patterns inside the synaptic region of the central complex. **A-C**: Patterns of Tyrosine Hydroxylase (TH) labelling of dopaminergic neurons depict weak labelling of fan-shaped body layers I and II, spot-like layering of ellipsoid body layers I-III, as well as projection pathways from the superior medial protocerebrum into the fan-shaped body (arrows), ventral projections into the ellipsoid body (arrows) and projections from the bulb into the ellipsoid body (arrows). **D-F**: Patterns of 5-hydroxytryptamine (5-HT) labelling of serotonergic neurons depict prominent labelling into layers II and III of the fan-shaped body, from projections in the superior medial protocerebrum (arrowheads), as well as showing spot-like labelling of the ellipsoid body layers I and II from ventral projections as well as dorsal projections (arrowheads). **G-I**: Fasciclin-II labelling of a subpopulation of columnar neurons across all lineages DM1-4 emerging into prominent labelling of layers II-IV of the fan-shaped body and all layers in the ellipsoid body. In addition, projections into the gall from the ellipsoid body are shown (arrowheads). Abbreviations: PB protocerebral bridge, FB fan-shaped body, EB ellipsoid body, NO noduli, MB-LO mushroom body lobes, BU bulb, DM1-4 dorso-medial lineage 1-4, GA gall. Scale bars equal 100 µm.

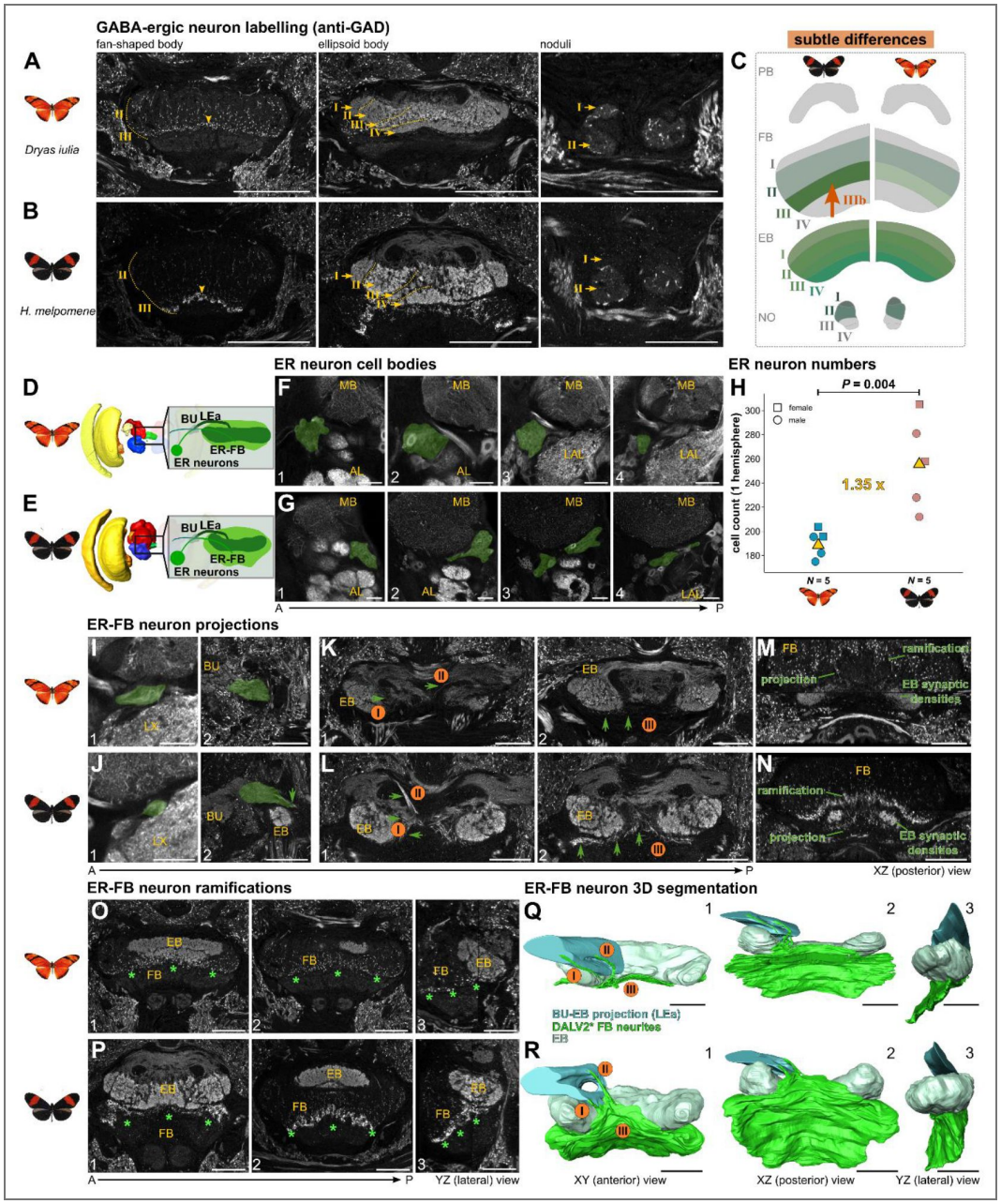

Figure 7. Anatomical and statistical analysis of GABA-ergic DALv2 lineage-derived ER neurons showing higher innervation of the FB in pollen feeding *Heliconius melpomene* versus *Dryas iulia*.

A-C: Patterns of GAD (glutamate decarboxylase) labelling of GABA-ergic neurons depicting spot-like labelling in the fan-shaped body layers II and III, complete labelling of the ellipsoid body and spot-like labelling of nodulus layers I and II. **D/E**: Location of the GABA-ergic cell group and its projections in focus relative to the brain. **F/G**: Position of cell bodies, nestled between the mushroom body lobes and antennal lobe at the anterior surface of the brain, along four different positions of the anterior-posterior axis ("1-4"). **H**: Quantification of cell body numbers in both species revealed a significant increase in *Heliconius*. **I/J**: ER neurite close to the cell bodies at two different positions ("1-2"). **K/L**: Projection of ER neurites into the central body, with a focus on the projections into the FB. "I/II" indicate two tracts that project ventrally and form a fibre that sits ventrally to the EB ("III") **M/N**: A perpendicular view onto the projections labelled with "III" show the relative position of the beginning synaptic EB neuropil as well as the ER projections and ramifications leading into the FB. **O/P:** Focus on the ramifications of the ER-FB neurons inside the FB at two different A-P axis points ("1-2"), as well as a lateral view ("3"). **Q/R:** 3D segmentations of the ER neurites with focus on the FB contributing portion, with three different viewpoints ("1-3"). Light blue depicts the massive projections into the light-grey labelled EB, with green showing the projections and ramifications into the FB. All immunostaining depictions are based on an anti-GAD labelling. Abbreviations: BU bulb, LEa lateral ellipsoid body tract, ER ellipsoid body ring neurons, MB mushroom bodies, AL antennal lobe, LX lateral complex, FB fan-shaped body, EB ellipsoid body. A anterior, P posterior. Scale bar equals 50 µm, except for the central body panels in A/B where it is 100 µm. See animated 3D segmentations and annotated stacks in file repository.

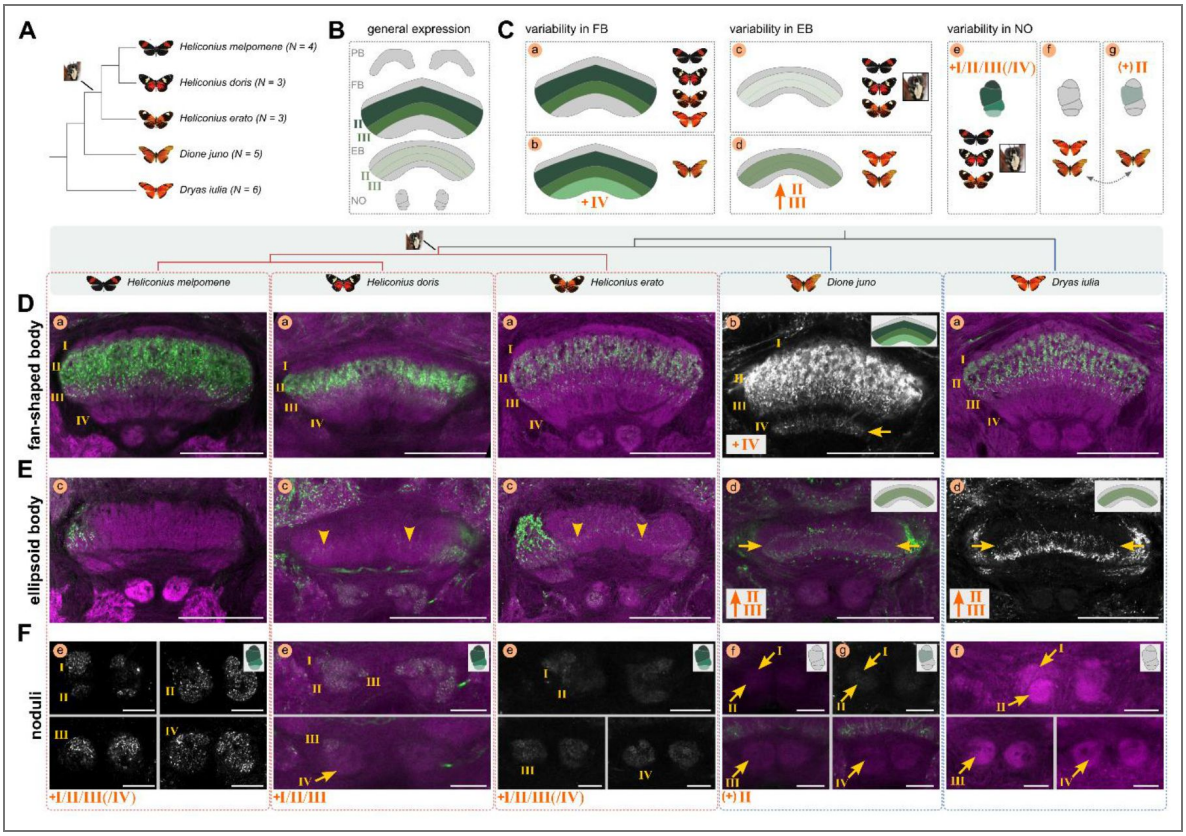

Figure 8. Anatomical analysis of Allatostatin A expression across five representative species of Heliconiini reveals variability consistent with behavioural innovations in *Heliconius*.

A: Summary of the dataset used to assess Allatostatin A variability, with the phylogeny of sampled species and indication of when pollen feeding evolved. **B**: General expression pattern of Allatostatin A that is present throughout all species. **C:** Schematic representation of the interspecific variation present in Allatostatin A expression in fan-shaped body, ellipsoid body and noduli, with major differences indicated in orange lettering. If consistent with a shift in *Heliconius*, this was indicated by the pollen feeding photograph. Lower-case letters correspond to figure panels in D-F, where this variability of expression is depicted. Note that *Dione juno* varies in its noduli expression even between individuals, hence the double-headed arrow. **D-F**: Variation in Allatostatin A expression (green or grey) across the five Heliconiini species. Synapsin was used as co-stain, depicted in magenta. Lower-case letters correspond to the schematic in c, with schematic depictions of the central complex neuropil in question indicated where consistent differences between species was identified. Arrowheads specifically point to difficult to identify expressions of Allatostatin A in the ellipsoid body of some species. Arrows point to differences described in the schematic and in text. Abbreviations: PB protocerebral bridge, FB fan-shaped body, EB ellipsoid body, NO noduli. Scale bars in D and E equals 100 µm and in F 25 µm.

innervations of fan-shaped body layer I and II. Layer I was only very faintly labelled, with arborisations leading back to cell bodies near the mushroom body calyx. These neurons might be homologs to neurons reported in the moth *Manduca sexta* [60]. We detected spot-like labelling of ellipsoid body layers II-IV, which are likely generated by neurons that project from ventral and dorsal locations that might include ER neurons with inputs in the bulb (Figure 6A-C), and/or neurons homologous to EXR2/TL5 neurons [51]. Within the constraints of the information provided in these stainings, the pattern of dopaminergic staining was highly conserved across species (Figure 6C).

To identify serotonergic neurons we used a 5-hydroxytryptamine (5-HT) antibody. Like in other insects [61], 5-HT staining revealed a prominent labelling of fan-shaped body layer II and weaker labelling of layer III through a small number of neurons in Heliconiini (Figure 6D-E). The cell bodies of these neurons are situated at the most posterior end of the brain, surrounding the protocerebral bridge and anterior sections of the calyx. Beyond the branches in the CX, these neurons seem to arborize inside the SLP and SMP. Layer II of the ellipsoid body was faintly labelled in both species. Particularly the pattern of strong layer II labelling was well conserved across other Heliconiini species (Figure S4C-D). Taken together, we did not observe any pronounced differences of serotonergic neuron expression across *Heliconius* and their non-pollen feeding outgroups (Figure 6F).

We also stained against Fasciclin II (Fas II), a cell adhesion molecule with broad neurodevelopmental roles that was previously used to reveal more specific detail in insect mushroom bodies [28,62], but that also showed interesting patterning in the CX. In contrast to the neurotransmitter stainings, this staining labelled a portion of columnar neurons of each group of DM1-4 lineages, i.e. a subset of the WXYZ tracts (Figure 6G-I) which resulted into prominent labelling of layer III and IV of the fan-shaped body as well as weaker labelling of layer II. In addition, we also observed very prominent labelling in the entire ellipsoid body, revealing all four layers, particularly in *Dryas iulia* (Figure 6G). The staining further revealed a tract that connects the ellipsoid body to a small region of the lateral complex, called the gall (right most panels of Figure 6G-H) [63]. As this tract is typical for EPG neurons, this suggests that Fas II stained the compass neurons in the Heliconiini ellipsoid body [57,64,65]. In summary, the observed patterns of these three stains reveal conserved details of anatomy across the Heliconiini.

GABA-ergic ER neurons increase in number, with increased innervation of the fan-shaped body in pollen feeders

We next explored variation in GABA-ergic neurons and neurons that express Allatostatin A, which reveal evidence of deviation from the general conservation described thus far. GABA-ergic antibody staining using an anti-Glutamate decarboxylase (GAD) antibody resulted primarily in staining of ER neurons which we focus on chiefly (Figure 7, Figure S4A-B). Generally, however, this antibody labels conserved features (Figure 7A-C), specifically, we detected spot-like labelling in layers II and III of the fan-shaped body with projections from the SMP and SLP (matching expected pathways between mushroom bodies and CX and these regions [21]), as well as layers I and II of the noduli with unclear, but anterior, origin.

Typical for GABA-ergic expression [66], the most dominant and conserved labelling was in all four layers, I-IV, of the ellipsoid body (Figure 7). Anti-GAD staining reveals a pattern where large portions of neural lineages are labelled and the whole cells, including somata and branches, are evenly marked. This allowed us to quantify even densely packed cell groups typical for insect neurons, such as the DALv2 neural lineage and resulting ER neurons which we focussed on next. To identify this cell group, we cross-referenced our labelling with previously published work [66]. This revealed a characteristic and very prominent labelling of the ellipsoid body by a cell group whose cell bodies are positioned anterior-laterally to the ellipsoid body, nestled between the antennal lobe and mushroom body lobes (Figure 7D-G). This well-characterized group of cells is usually referred to as R/ER (ring) or TL2/3 neurons (tangential neurons of the ellipsoid body), while the lineage they are produced by is referred to as dorsoanterior lateral ventral 2 (DALv2) (or anterior ellipsoid body; EBa1), and their tract is named either LEa (lateral ellipsoid fascicle,

anterior part) or IT (isthmus tract) [45,66,67]. Here, we refer to these neurons, as well as those neurons projecting to the fan-shaped body (GU neurons in [66]), as ER neurons due to their common developmental origin [45,66] and to simplify anatomical descriptions. The projection and ramifications inside the ellipsoid body were conserved across Heliconiini. Indeed these cells show strong conservation across insects [66], as they are an essential part of the anterior visual [68] and sky compass pathway [46], receiving visually guided signals from the AOTU and projecting those to the ellipsoid body (Figure 7D-F).

While we identified very strong conservation of projections to the ellipsoid body, we noticed a pronounced difference in a portion of projections leading into the fan-shaped body and a strong difference in signal inside layer III in our two focal species, *H. melpomene* and *D. iulia*, as well as other representatives of the Heliconiini tribe (Figure S4A-B, Figure 7). To understand how these differences could have occurred, we quantified ER neuron numbers in our focal species, and identified a significant difference, reflecting a 35% increase in *Heliconius* ($t = 4.221$, $P = 0.004$; Figure 7H). Most ER neurons will still produce the heavily conserved innervation of the ellipsoid body, but the additional neurons in *Heliconius* likely produce the increased ramifications we observed in layer III of the fan-shaped body.

To illustrate this connection, we next disentangled the projections that lead to the ellipsoid body from those that lead to the fan-shaped body. The whole cell group projects past the gall (GA) and lateral accessory lobe (LAL) to build a large conflation point constructing the bulb (BU) neuropil together with groups of neurons that project to it from the AOTU [45,46] (Figure 7I-J). The projection, the LEa/IT, leads further into the central body where most neurons enter and terminate in the ellipsoid body (with a slightly modified shape of this projection between the two Heliconiini clades, Figure 7Q/R-1). In both species, we saw two major projections leading into the fan-shaped body, following a projection ventrally and posteriorly, away from the ellipsoid body (Figure 7K/L and Q/R). The first projection "I" enters slightly more ventrally but originates laterally inside the LEa. Projection "II" enters medially and slightly more dorsally. Both then construct a projection line ventrally to the ellipsoid body (Figure 7K/L 2 and Q/R; "III"). Observing this pattern from a ventral view illustrates how these projection points lead to the actual ramifications inside the fan-shaped body (Figure 7M-N). Most importantly, the ramifications build a very thin and faint line in the non-pollen feeding outgroups (Figure 7O/Q), but a very prominent labelling of layer III of the fan-shaped body in *Heliconius* (Figure 7P/R). Whether these ER neurons solely branch in the fan-shaped body, as shown for GU neurons elsewhere [66] or have additional side branches entering the ellipsoid body is not clear.

To carry visual information to the ellipsoid body, ER neurons arborize with neurons projecting from the AOTU in a conspicuous and small neuropil called the bulb (Figure S5). We wanted to examine whether divergence in ER neuron number and changes in fan-shaped body projections are concurrent with changes in bulb size, and potentially bulb microglomeruli number (Figure S5). We generated high resolution images of the bulb to determine its size (Figure S5 C-F), and 3D segmented seven microglomeruli per individual with which we generated an extrapolated approximation of total microglomeruli number by dividing bulb volume with average microglomerulus volume. This was necessary as most microglomeruli were not discernible from each other (Figure S5 G-H). Importantly, we did not detect any significant species, nor sex differences in this dataset (Figure S5 I-K). In addition, ER neuron number did not predict bulb size, or microglomeruli measures (Table 1).

In summary, we observed a conserved origin and projection pattern of GABA-ergic ER neurons in the ellipsoid body and a conserved size and microglomerular count in the bulb, but did detect a divergence in the number of ER neurons and corresponding size of their innervation in fan-shaped body layer III.

Variation in Allatostatin A staining indicates species differences in noduli and central body layers

Neuropeptides are often co-expressed with neurotransmitters to generate flexibility in neural circuits [69,70]. Allatostatin A is a prominent example of these short peptides, where co-expression with serotonin, for example, might generate such flexibility in the response to sensory cues [71]. We labelled Allatostatin A expression with a Dip-allatostatin antibody, which revealed labelling of the neuron terminals near the synapses, as this is where the neuropeptides are transported to upon translation. Due to the species-dependent [72] and state-dependent nature of neuropeptide expression and potential variation in expression levels [73,74], we examined Allatostatin A expression in five different species (*H. melpomene, H. erato, H. doris, Dryas iulia, Dione juno*) and 3-6 individuals each (Figure 8A), with a consistent protocol throughout.

Across all species and individuals, we consistently identified an absence of staining in the protocerebral bridge and a very strong labelling in layers II and III of the fan-shaped body, with particularly high expression levels in layer II (Figure 8B). However, we observed considerable species-consistent variation in the remaining layers of the fan-shaped body, ellipsoid body and noduli (Figure 8C):

A. In the fan-shaped body we found broad and consistent expression in layers II and III across *Heliconius* and outgroups (Figure 8D). In *Heliconius doris*, Allatostatin A was also expressed in layer IV, with slight variation in terms of strength between the five individuals (compare a to b in Figure 8D).
B. In the ellipsoid body, we only detected strong expression in an area likely to be layers II and III in *Dione juno* and *Dryas iulia*, which are outgroup genera and do not feed on pollen, while we never saw strong expression in *Heliconius* (compare c to d in Figure 8E). In some cases, there was no expression at all (*Heliconius melpomene*), while in case of *Heliconius erato* and *doris*, we only detected very weak and inconsistent expression (arrowheads in Figure 8E). Hence, these inter-specific differences reflect the divergence between pollen-feeding *Heliconius* and outgroups (Figure 8C).
C. Mirroring variation in general anatomy (Figure 4C-D), expression of Allatostatin A in the noduli varied across species. We only saw prominent expression in *Heliconius* (Figure 8F-e). Outgroup Heliconiini species always showed an absence of Allatostatin A expression (Figure 8F-g) or, in case of *Dione juno*, faint expression in layer II of the noduli was observed in only two of five individuals. Again, any pronounced differences were linked to the split between pollen-feeding *Heliconius* and outgroups (Figure 8C).

We also have indications of frequent patterns of co-expression between neuropeptides and neurotransmitters [69,70], as Allatostatin A and Serotonin were expressed in fan-shaped body layers II and III (compare Figure 8B to Figure 6F), and dopamine in layer II (Figure 6C). The expression patterns we observed in Heliconiini are partially conserved when compared to *Drosophila*, and potentially with expression patterns in *Schistocerca* [69,71]. Moreover, Kaiser et al. [75] identified Allatostatin A expression in three fan-shaped and two ellipsoid body layers in the honey bee brain, which seems particularly similar to the expression patterns that we observed in *Dryas* and *Dione*. While they state that the ellipsoid body expression patterns seem to originate from populations of tangential neurons, the fan-shaped body expression pattern we observe in Heliconiini is very likely generated by columnar neurons [75]. In our data the columnar neurons were indeed labelled in some individuals, though it was not possible to connect labelled cell bodies to their resulting expression in the central body.

In sum, we identified pronounced variation in Allatostatin A expression, which contrasts with the conserved patterns observed for serotonergic and dopaminergic neurotransmitters. Interestingly, some of these differences were consistent between multiple *Heliconius* species and multiple outgroups, potentially reflecting differences that occurred alongside the origin of pollen feeding, derived spatial foraging behaviours, and mushroom body expansion.

Discussion

Heliconius butterflies possess a unique dietary innovation, associated with derived foraging behaviours that are dependent on spatial memory and navigation. This evolutionary shift in learning and memory has previously been linked to a major expansion and specialisation of the mushroom body [28,29,36], but its impact on downstream pathways that must interact with mushroom body outputs to coordinate navigation and goal orientation behaviours has not been assessed previously. In this study, we identified that the volumetric expansion in the mushroom bodies in *Heliconius* butterflies did not occur in concert with volumetric changes in central complex neuropils, AOTU or the POTU (Figures 1-2), which provide this function. We determined a largely conserved pattern of substructures (Figures 4-6), but did identify evidence of subtle, but highly specific patterns of divergence in the central complex of *Heliconius*, with an increased number of ER neurons, which innervate a specific layer of the fan-shaped body (Figure 7), and different expression patterns of the neuropeptide Allatostatin A, particularly in the noduli (Figure 8). Below, we discuss the potential functional and evolutionary implications of this overall conservation, and specific instances of divergence.

Evolutionary implications of volumetric conservation

While the lack of volumetric change inside the central complex neuropils, as well as the AOTU and POTU, contrasts dramatically with mushroom body evolution in Heliconiini, it is more consistent with the overall impression that the central complex has a largely conserved structure across all pterygote insects [55]. Conservation of gross anatomy may indicate that it is not necessary to change the central complex, AOTU and POTU substantially to modify cognitive processes in such a way to allow spatial foraging to occur. Indeed, volumetric conservation is important as it indicates probable conservation in the number of overall synapses, and hints at conserved terminal axonal and dendritic branches as well as glial processes, which are important domains of adaptive change in neural circuitry [1,3,76]. However, what these synapses do and to which cell types they belong to is not always reflected in gross anatomy, which means that these systems might indeed be meaningfully modified, just not in ways that are reflected by volumetric differences [3,77,78]. In effect, any inferences of volumetric conservation may obscure many more fine-scale differences, such as some identified here (Figure 7 and 8), but potentially many more that have yet to be examined in an evolutionary framework [1,3,78].

Implications of central complex circuit logic on evolutionary constraints and adaptability

Evolutionary constraints, which are any aspect of a system's biology that limits the response to selection, are hypothesized to shape brain and neural system evolution by determining the landscape of adaptability in those systems [4]. While developmental constraints imply that conserved developmental programs reduce the available potential outcomes, functional constraints imply that in order to fulfil essential and ancestral functions, large parts of many neural circuitries must be conserved [4]. The considerable data available on the circuitry of the insect central complex offers possible explanations about how a dual pattern of conservation and divergence inside the central complex may come about.

The central complex is mostly made up by two dominant cell groups: columnar and tangential neurons. Each contain various subgroups with specific projection patterns, with other, multi-columnar, neuron types representing a relatively small proportion of cells [54,55]. Columnar neurons offer insights into developmental as well as functional constraints, while tangential neurons may be interpreted as this neural system's main axis of adaptability. Columnar neurons interconnect the different central complex neuropils and connect to the lateral complex [53,57,79,80], where specific columnar types (PFL neurons) transfer information to descending pathways that relay navigational motor responses to the thoracic ganglia. Importantly, through their small projection fields, they innervate only small portions of the protocerebral bridge, fan-shaped body and ellipsoid body, and thus divide the central complex into vertical columns that, together with

horizontal layers, create an orthogonal array of subdivisions [53,57,79,80]. This array is not only essential to central complex circuitry but offers a very clear example of how structure is translated into function. The head direction circuit, formed by neurons branching in the protocerebral bridge and the ellipsoid body, illustrates this point particularly well. Here, many circuit elements are conserved even when structures vary markedly in shape, such as between toroid or bar-shaped ellipsoid bodies [14,17,21,50,53,79–83], because each vertical column represents an equal portion of an animal's 360° space [11,21,84]. This universally required arrangement imparts cognitive demands on this circuit, thereby placing functional constraint on possible axes of variation, such as projection patterns, ramification size and synaptic connectivity. This ultimately limits the variability of particular types of columnar neurons. Moreover, all columnar neurons are, per hemisphere, constructed by only four neural lineages, called DM1-4. These neural lineages seem to be largely conserved across insects, even in terms of absolute cell number [33,59,85,86] which indicates considerable constraint in their developmental programs, and also implies that modifying the number of columnar neurons in a substantial way would neither be necessary nor useful to retain functionality. Instead, changes in the relative distribution of specific neuron types that occupy each column may be a more functionally malleable axis of variation across species.

The adaptability of central complex function may instead be more likely to occur in tangential neurons [54,55], such as the ER neurons that we characterized more closely. Tangential neurons connect other brain areas and other subcircuits to the central complex, thereby dividing the central complex into horizontal layers. These neurons may harbour more adaptability as they essentially "plug in" information of context-dependent cues, such as different sensory modalities and internal states, from other brain regions, including the mushroom bodies, to the conserved array of columnar neurons [21,45,51]. Variability in these connections are also reflected in a broader developmental basis, where 18 different neural lineages are involved in the generation of tangential neurons [45]. As these neurons have a much more diverse developmental origin, location in the brain and independent function [45,51], we speculate that input strength, ramification size and synaptic changes can occur partially independently to the columnar neurons.

Layers that are formed through these tangential neurons, particularly in the fan-shaped body, are thought to be one of the most variable domains in central complex circuitry [55], for which we here offer a rare comparative example by identifying an increased innervation of fan-shaped body layer III in *Heliconius* butterflies, which rely on spatial memory to direct foraging behaviour (Figure 7). Indeed, the fan-shaped body at large is involved in selecting and generating goal directions, and a subsequent comparison to signals encoded by the head direction circuit will then result in a specific navigational response [19–21]. To allow navigation to a specific goal, the fan-shaped body receives information related to translational movements via the noduli [17,87,88], as well as a multitude of other direct and indirect inputs from mushroom body output neurons for example, which encode memory-specific signals, and other internal state information [22,45,89]. As such, it may vary more across species, reflecting the specific behavioural repertoires of a lineage, to provide integration that often depends on shifts in sensory cues and increased reliance on internal motivation [55], which may be closely linked to ecological need. Indeed, a columnar architecture is often less obvious in the fan-shaped body than in the ellipsoid body and protocerebral bridge [79,80], potentially reflecting its necessary functional variability [21,33,52,55].

Implications of fine differences in a conserved central complex circuit

Our neuromodulator labelling permitted us to take a closer look at potential divergent traits, and interestingly these match to the areas of the central complex where adaptive variation could be expected to occur, i.e. the fan-shaped body and noduli [21,55]. While significant parts of the neurotransmitter system in Heliconiini seem conserved (Figure 6), matching previous observations [28], we identified quantitative differences in GABA-ergic ER neurons, as these occurred in higher number in *Heliconius*, and produced an increased innervation of fan-shaped body layer III (Figure 7). These results shine light on the much less examined portion of ER neurons that innervates the fan-shaped body but in a direct comparative setting. *Drosophila*

connectome data [21,45], as well as immunohistochemical data across insects [66], indicates that the DALv2 lineage and the resulting ER neuron population always has a conserved portion of cells that connect to the fan-shaped body, but potentially varying amounts relative to the whole ER neuron population across insects, even if this is only 5% in the case of *Drosophila* (Figure 1 in [45]). Indeed, the projection pattern of the fan-shaped body projecting neurons in *Heliconius melpomene* closely resembles their homologous counter parts in *Drosophila*, despite their distant phylogenetic relationship (Figure S4 in [45]). Our data also indicate that this portion of cells could be subject to a significant amount of evolutionary adaptability, particularly in terms of cell numbers. This is corroborated by substantial differences in fan-shaped body ramification patterns across insects [66].

In addition to the ER population and its arborisations in the fan-shaped body, we also closely examined the bulb (Figure S5). The bulb is made up by large synaptic complexes, or microglomeruli, constructed primarily by TuBu neurons that enter the bulb from the AOTU and ER neurons that connect to these TuBu neurons and project any modified signals into the ellipsoid body [79,90–93]. We did not identify any species differences in several variables of bulb anatomy (Figure S5), despite an increased number of ER neurons. This supports our hypothesis that the portion of ER neurons that is increased in *Heliconius* might partly be those which project to the fan-shaped body, without arborizing inside the bulb at all. Alternatively, these ER neurons would still arborize in the bulb, but to the same number of TuBu neurons, thus not requiring increased number of synapses which might be reflected in the variables that we examined, but then branch into the fan-shaped body. Either way, our finding of conserved bulb architecture narrows down the area of change considerably.

This GABA-ergic ER neuron population and related projection differences, despite their relatively subtle appearance, may have functional and behavioural relevance. In a recent model [94], "vector memory neurons" synapse onto and inhibit valence signals in fan-shaped body columnar neurons. Through this connection, a current heading direction could be inverted, inducing the return of a path-integrating animal to its original position [94]. This could be an important element in the context of navigational demands placed on *Heliconius* butterflies, who need to reliably memorize and navigate to and from a nocturnal roost site during their spatial foraging navigation [32,95]. An increased portion of inhibitory vector memory cells, in this case ER neurons projecting onto "integrator neurons" in fan-shaped body layer III, could fulfil these demands in a more precise, more parcellated, manner.

In addition, we also detected substantial, but species-specific, variation in Allatostatin A labelling in the central complex. Across the insect brain, Allatostatin A has broad roles in the regulation of feeding, development, alternation of activity and sleep as well as learning [73,96–99]. We described four patterns of variation (Figure 8C), two of which are consistent with a divide between the pollen feeding *Heliconius* and outgroup genera. While some of these differences are difficult to interpret, the expression of Allatostatin A inside large parts of the noduli in *Heliconius* is intriguing. The noduli are the target of several tangential neurons, termed TN1 and TN2, carrying information about self-motion cues such as translational optic flow to estimate distance [17,87,88]. It is possible that Allatostatin A is expressed alongside neurotransmitters to co-regulate the activity of specific populations of such tangential neurons or, indeed PFN neurons that receive information by these neuron populations and then project these to the fan-shaped body. Interestingly, the central complex of bumblebees, like *Heliconius*, an allocentric spatial forager, houses twice the amount of PFN neurons than the central complex of fruit flies [33]. This could improve spatial foraging by integrating motion and locomotory information with compass information to induce novel goal directions [17]. Moreover, spatially foraging Hymenoptera harbour modifications of their noduli, a "nodulus cap", likely being a unique structural adaptation to specific computational needs surrounding navigation [33,55]. Hence, while there is currently no direct evidence indicating how the behavioural and cognitive challenges associated with long-term spatial memory in *Heliconius* are functionally connected to the changes in Allatostatin A expression in the central complex (Figure 8), there is comparative evidence in other foragers suggesting this site may be functionally important for spatial behaviours.

Information pathways for spatial foragers into the central complex

Like in other insects [66], GABAergic ER neurons in Heliconiini butterflies mostly have synaptic input in the bulb and transfer information into the central complex. ER neurons projecting to the ellipsoid body are part of a visual compass pathway and encode external orientation cues, such as the sun azimuth, polarised skylight information and panoramic scenes [15,16,82], information that would be especially relevant during spatial foraging of *Heliconius* butterflies. ER neurons carry visual information to the ellipsoid body, where they inhibit the head direction network [100]. Through Fas II staining (Figure 6), we were able to identify neurons that interconnect the ellipsoid body with the gall and the protocerebral bridge, and that are likely the homologues of EPG neurons in the Heliconiini central complex. Thus, like in other insects, the Heliconiini central complex is equipped with a head direction network that encodes a current head direction of the butterflies. Compass information of these EPG neurons is likely transmitted in the protocerebral bridge via Δ7 neurons to PFN neurons, a type of neuron that has also reported in several insects, including butterflies [53,57,79]. Fruit fly PFN neurons are involved in transforming the heading signal into a body-invariant travelling direction in the fan-shaped body [87,88]. Lepidopteran PFN neurons likely have the identical function.

Importantly, we also found that some ER neurons bypass the ellipsoid body and give rise to dense branches within distinct layers in the fan-shaped body (ER-FB) and an increased innervation in spatially foraging *Heliconius*. In addition, our GAD staining also revealed GABA-immunoreactivity in arborisations in the SMP, a major target region of mushroom body output neurons (MBONs) carrying modified synaptic input from Kenyon cells to other areas of the brain [12]. Although we cannot undoubtedly assign these GABA-ergic arborisations to the ER-FB neurons, additional branches of homologous cells have been previously described for *Drosophila* ER-FB neurons [45]. It is therefore plausible that specific mushroom body output signals of the massively enlarged mushroom bodies of *Heliconius* species connect to an increased portion of ER-FB neurons, subsequently projecting into the fan-shaped body. Indeed, through dye injections, we also found that neurons of the SMP/SLP project to the fan shaped body (Figure 5), similar to what has been described in the Monarch central complex [57].

In addition to its classic attributes of associative learning and memory, mushroom bodies produce and encode familiarity of visual scenes, which is an essential information if visual scenes and olfactory signals are used to associate specific environments with a “homing vector” during trap-lining or other forms of spatial foraging. How familiarity is integrated into the navigational circuit of the central complex is largely unknown [101] but our results support recent models suggesting that familiarity cues from the SMP/SLP could provide valence information based on memorized visual scenes and olfactory cues that gate goal direction navigation in the fan-shaped body, a mechanism proposed to exist in *Drosophila* [22]. In this context, ER-FB neurons could play a major role in modulating the signals of MBONs in the SMP/SLP and/or in the fan-shaped body, before they are used to produce steering signals in the fan-shaped body. Such a mechanism would allow *Heliconius* butterflies to store and recall a number of vectors in the fan shaped body and, thus, would establish the neural correlate of a navigation strategy akin to trap-lining [32].

Conclusion

By leveraging the unique biology of *Heliconius* butterflies and their close phylogenetic relationships with outgroups that lack their behavioural specialisations, we provide a rare example of evolutionary divergence of the central complex in fine-anatomical detail among closely related species. Our study has identified areas of the central complex circuitry where changes may occur to modify circuitry in such a way to facilitate the evolution of spatial foraging. The central complex is an intriguing system to study circuit divergence, exactly because it is generally so highly conserved, and because its structure is directly translated into its function [55]. In light of this general conservation, any fine differences that are identified are potentially easier to connect to specific behavioural traits compared to more divergent circuits. The model system of

spatial foraging adaptation in Heliconiini butterflies highlights very different ways to modify circuitries in the two integration and navigation centres, the mushroom body and central complex [28,101]. It is therefore uniquely suited to be examined further to investigate the precise circuitry underpinnings of constraints and adaptability [3].

Material and Methods

We have derived our results from two datasets with different origins, which we describe below for each. Data which is relevant to figures and statistics is deposited at *https://doi.org/10.5281/zenodo.15304965*.

Dataset for large-scale volumetric analyses

All the 307 individual Heliconiini butterflies used in the large-scale statistical analysis (Figures 2-3 and S1-S3) were wild-caught and are part of the same dataset used in a previous study [29]. Here, we segmented the neuropils of the central complex (CX) as well as the anterior (AOTU) and posterior optic tubercule (POTU) and used the openly available data for the mushroom body and other measures to generate a collective volumetric dataset for 307 individuals of 41 species of Heliconiini for the CX, AOTU and POTU as well as the mushroom body (MB) and central brain volume (CBR), the basis for the allometric control variable. Note that we did not have noduli (NO) sizes for all individuals due to some inconsistent image quality, which is why we excluded NO size in the within neuropil analysis as predictor of all others and only used it as dependent variable (missing values in Figure 3).

Dataset for small-scale fine-anatomical analyses

Individuals used for finer scale data analysis (Figures 4-8 and S4-S5) overlapped partially with butterflies used previously [28], and as a result, rearing procedures, fixations and stainings were highly similar or identical. In short, pupae of Heliconiini butterflies were ordered from commercial suppliers (The Entomologist; *https://butterflypupae.com/* or Costa Rica Entomological Supply; *www.butterflyfarm.co.cr*). They were then attached posteriorly to a microfibre cloth in a pop-up cage. After eclosion, they were given IDs, marked on their forewings, to later identify their age when sampling. They were reared in 2 x 2 x 2 m mesh cages at 26°C, 80% humidity and a 16 h/8 h light/dark cycle, with *ad libitum* feeding consisting of flowering *Lantana* plants as pollen and nectar supply and artificial feed containing 20% sugar and 5% critical care formula (VETARK, Winchester, UK) in water. All images displayed in figures are supplied at *https://doi.org/10.5281/zenodo.15304965*, with a list of which figure refers to which file in Table 2.

3D segmentations of volumetric dataset

3D segmentations of the CX, its neuropils as well as the AOTU and POTU were performed using Amira Version 2020.2 and Version 5.4.3 (effects of version and experimenter were ruled out statistically). For the segmentations, we used the identical procedure as previously described [29]. First, to correct for axial aberrations due to differences in the refractive indices of air and the mounting medium of the samples of the volumetric dataset, we used a corrective scale factor of 1.52 on the z-dimension as determined previously [102]. We then used the segmentation editor on a grey image stack of labelled brain to mark each neuropil through the brush or wand tool in approximately every 10 slices for larger neuropils and 3-5 slices for smaller ones, using interpolation subsequently. Manual segmentation and interpolation was verified using all views (xy, yz, xz) of the segmentation editor. The selection was smoothed in each view for most neuropils, except for the small neuropils, i.e. the POTU and NO. Smoothing of the 3D surface of reconstructed neuropils was only performed for visual representations such as in Figure 1. Here, other neuropils, such as the mushroom body, antennal lobe and visual neuropils were segmented identically as described in [102].

Statistical tests of volumetric dataset

All tests were performed with R 4.3.1 in R Studio 2023.06.0 [103,104]. Packages used and full results are found in Table 1, while the script is found at *https://doi.org/10.5281/zenodo.15304965*. To assess patterns of variation in this species-rich dataset we used phylogenetically corrected GLMMs (general linear mixed models) based on Bayesian statistics using *mcmcglmm* [105]. We always ran every model twice and compared effects by using the Gelman Diagnostics criterion. We checked for their common convergence through analytical as well as visual means and determined covariance values below 1.1 as acceptable. Priors were set for residuals and random effects with a univariate inverse-Wishart distribution (V = 1) and a degree of belief parameter (nu) of 0. We sampled 500,000 iterations with a burnin of 10,000 and sampling each 500 iterations. We used the phylogenetic tree published with Couto et al [29]. We compared to null models when testing the effects of interactions of pollen feeding/clade membership to volumes using the difference and extents of DIC. In all cases, if the DIC of the test model was larger than null, the differences were miniscule.

To assess differences in evolutionary rate in CX, AOTU and POTU compared to what has been determined in the MB by Couto et al [29], we used an identical approach. We calculated species averages and used a multirate Brownian model assumption to calculate rates. CX rates were regressed to rCBR rates. Residuals were then plotted with colour coding according to the original MB plot to assess MB and CX differences comparatively.

To assess differences within tested structures (CX neuropils, AOTU, POTU) we performed *mcmcglmm* models with one structure as dependent variables and all others as independent variables. In case of the NO, we only used data points where NO data was available, thus reducing the amount of data points tested. To account for multiple testing effects in these within-effects tests, we multiplied the *P* value by four for the main within tests as each structure was included four times in other tests. For the *posthoc* effects tests of the significant results we multiplied *P* values by the number of significant relationships, i.e. 10.

We tested for sex effects and provide these results in the Supplemental Text. In short, while we did identify some significant effects of sex, they were small in effect size and do not impact the results presented in the main text. Hence, we report them in Figure S1 and account for variation of sex in all models, but – in absence of any prominent hypothesis – refrain from any discussions around them here.

Antibody use and characterisation for fine-scale analysis

All antibodies used in this study are described with information about origin and usage in Table 2. All antibodies used are commercially available, their specificity carefully assessed and widely established and have revealed conserved expression patterns previously [60,61,66,71,96]. We used synapsin, acetylated tubulin and HRP as structural markers. The combination of tubulin and HRP reveals the whole neuronal structure, from cell soma to synaptic endings [28]. We selected a series of markers for neuromodulators that are typical labels of fine structures in the CX [72] to reveal series of specifically labelled neurons. These were antibodies against Glutamate decarboxylase (GAD) to label the neurotransmitter γ-aminobutyric acid (GABA), Tyrosine hydroxylase (TH) to label the neurotransmitter dopamine, Serotonin or 5-hydroxytryptamine (5-HT) and the neuropeptide Allatostatin-A. We also used a Fasciclin-II antibody as selective label only, as it previously revealed specific populations of neurons relevant to the CX [28].

Dissection, fixation, immunostaining and bulk injections for fine-scale analysis

These procedures were close to identical to our previous study [28] and are highly similar to published protocols [29,106]. Butterflies with ages ranging from 3-5 days were decapitated following a short cold-anesthesia. Their antennae, proboscis and palps were removed and the head was pinned with anterior to the top. First, the head was opened by removing the interocular cuticle up to and including the antennal roots. We then exposed the head and brain to the fixative *in situ*,

fixed the brains for 22 h at room temperature on an orbital shaker, and only subsequently, removed the brain from the head capsule. We used HBS (HEPES-buffered saline; 150 mM NaCl; 5 mM KCl; 5 mM $CaCl_2$; 25 mM sucrose; 10 mM HEPES) as dissection medium. We used 1% Zinc-Formaldehyde (ZnFA; 18.4 mM $ZnCl_2$, 135 mM NaCl, 35 mM sucrose, 1% formalin) as fixative, as described previously [106], having a less stark effect of introducing aberrations in the tissue. After fixation and dissection, all brains were subjected to a two hour incubation in Dent's solution (80% Methanol, 20% DMSO) with a subsequent rinse and storage in methanol at -20°C. We rehydrated brains in a descending methanol series (90%, 70%, 50%, 30%) diluted in 0.1 M Tris-HCl (pH = 7.4), by washing them in each dilution for 10 min, and a final wash in 100% 0.1 M Tris-HCl.

We sectioned brains at 80 µm using a Leica Vibratome VT1000-S (Leica Biosystems, IL, USA) with speed and frequency set to 5. The brains were prepared for sectioning by embedding the rehydrated brains in 5% low melting-point Agarose (#16520-050, ThermoFisher Scientific, MA, USA) and fixing them on a magnetic disk holder using cyanoacrylate glue, maintaining a non-tilted anterior-posterior vertical axis as much as possible.

Immunostaining was performed as reported previously. We used PBS-d (0.1M PBS [BR0014G, ThermoFisher Scientific, MA, USA] with 1% DMSO) as wash buffer, and started with a rinse subsequent to sectioning. We then performed a 30 minute permeabilization wash with permeabilization buffer (PBS-d and 2% Triton-X-100), rinsed once again with PBS-d and then started blocking using 5% of NGS (normal goat serum, G9023, MERCK, Germany) in PBS-d for 2-4 hours. We then applied the first antibodies with the appropriate dilution (see Table 2) in blocking buffer and incubated them for three days at 4°C on an orbital shaker. We then rinsed the brain sections once and washed them three times, for 30 minutes each, with PBS-d. Secondary antibodies were diluted in blocking buffer (see Table 2) and incubated for three days at 4°C on an orbital shaker. This was followed by a rinse in PBS-d and a 45 minute incubation of DAPI (1:1000) in water with 0.2% Triton-X-100. This was followed again by a PBS-d rinse and four 10 minute washes, and a final wash in PBS for one hour. We then transferred brains to 60% glycerol in PBS overnight for approximately 12-16 hours at 4°C or 2-4 hours at room temperature. Brains were then transferred to 80% glycerol for an hour and mounted on frosted object slides (J1800AMNZ, ThermoScientific, MA, USA) covered with #1.5 size coverslips and sealed with nail polish.

In addition to immunostainings, we also made use of a dextran injection into the superior medial and lateral protocerebrum (Figure 5). This injection followed procedures described elsewhere [29] and were exactly performed as in Farnworth et al [28]. Butterflies were secured in custom-made holders having a plastic collar around the cervix, with a waterproof barrier created by using low melting point wax around the head to prevent leakage of ringer solution (composition: 150 mM NaCl, 3 mM $CaCl_2$, 3 mM KCl, 2 mM $MgCl_2$, 10 mM HEPES, 5 mM Glucose, 20 mM Sucrose). We then exposed the dorsal region of the brain under the ringer solution and under filtered illumination, inserted the tip of a pulled glass capillary (G100-4, Warner Instruments, CT, USA), loaded with crystals of fluoro-ruby (dextran-tetramethylrhodamine: 10,000 MW, D1817, Thermo Fisher Scientific, MA, USA) mixed in 2% bovine serum albumin (BSA), into the cortical region of the brain. The capillary tip was held inserted for a few seconds. Subsequently, the head was covered with fresh ringer solution and kept overnight in a dark and humid chamber to facilitate dye diffusion. After incubation, the brain was dissected out, fixed in ZnFA, and immunostained with anti-SYNORF1 (3C11, Developmental Studies Hybridoma Bank, University of Iowa, IA, USA) following the same standard procedures described above and elsewhere [29,106]. After immunostaining, the brain was exposed to a series of increasing glycerol concentrations (1%, 2%, 4% for 2 hours each, and 8%, 15%, 30%, 50%, 60%, 70%, 80% for 1 hour each) in 0.1 M Tris buffer with 1% DMSO, before complete dehydration with three consecutive washes in 100% ethanol (for 30 minutes each) and embedding in methyl salicylate (M6752, MERCK Sigma Aldrich, MA, USA).

Imaging and image analysis for fine-scale analysis

We used a Leica SP8 (Leica Microsystems) and a 20X air objective (20X HC PL APO CS2, NA = 0.75) and for high-detail imaging a 40X oil objective (40x HC PL APO CS2, NA = 1.3) for the GABA-ergic labelling of the CX and a 60X oil objective (63x HC PL APO CS2, NA = 1.4) for bulb imaging. We

applied a 65 mW Ar laser, a 20 mW DPSS yellow laser and a 50 mW 405 nm diode laser to excite Cyanine-2 linked signal, Cyanine-3 linked signal and DAPI, respectively. Fluorescence signal was scanned using Hybrid detectors for Cyanine-2/3 and a PMT detector for DAPI. We used line averaging of 2-3, while using bidirectional scanning at 600 Hz with a resolution of at least 1024×1024. To calculate pinhole sizes, we used either the average of all emission maxima in use or the smallest emission maximum and set AU = 1. We then applied the system optimised z-slice size and linear Z compensation where necessary. Using the edge we cut into the agarose gel before slicing, we identified the same hemisphere consistently.

Image processing, 3D segmentation and annotation for fine-scale analysis

To generate accurate 3D segmentations in our fine-scale anatomical analysis, we corrected for axial aberrations due to refraction index differences between air and the mounting medium of 80% glycerol [107] using a correction value of 1.22 determined previously when using the 20X air objective [28].

We used Fiji 1.54 [108] and the included standard tools to modify brightness/contrast and orientation in all axes. We used an identical procedure described in [28] to generate a merged whole brain picture from brain slices, which in essence was based on creating concatenated stacks in Fiji with identical orientations, and then compensating for changes in both X and Y, using Amira 3D 2021.1 (ThermoFisherScientific, MA, USA) and its module *AlignSlices* in the first channel. Using *AlignSlices* on the second channel, we then used the first aligned channel as reference, enforcing identical shifts in X-Y in both channels.

The CX and associated parts in Figures 4 and 7 were segmented using the *labelfield* module and manual segmentation in approximately every 5-10 slices (2.5-5.5 µm) combined with interpolation. Interpolated segmentations were corrected in all views available. The selection as well as the segmentation was smoothed (value of 4 in all axes). To generate a surface view, we used constrained smoothing at a level of 3.

To segment the bulb, we created high resolution images and were particularly careful to only segment the area of the bulb that comprised large synapses/glomeruli, excluding parts of the LEa/IT projection. This was essential, because we relied on extrapolating the total number of microglomeruli from a subset of segmented microglomeruli and the total volume that contained microglomeruli, which means any section containing tracts and not glomerular structures would skew the estimated total number of microglomeruli. Extrapolation was necessary, as not all microglomeruli were visually discernible. We achieved an unskewed bulb volume by leaving out dense pieces of tubulin-positive tract material. We segmented seven microglomeruli per individual from the posterior section of the bulb, where they were most clearly visible, to get the most comparable impression across individuals and species. We then calculated average microglomerulus size and divided this by bulb volume to determine an approximation of microglomeruli number. To determine quantified patterns with these bulb metrics, we performed standard linear regressions in R. To determine ER neuron numbers in Figure 7, we counted cell bodies of one hemisphere manually, and performed standard linear regressions in R. We used Inkscape (*https://inkscape.org*) to generate all figures.

Supplement

Supplemental Text

To determine whether sex should be merely a control variable in subsequent testing or whether there were effects examinable for closer inspection, we determined a logical nested model design first (model a with only sex as test variable, b with sex and genus effects, c with their interaction), generated MCMCglmm models, and compared the DIC. Using the simplest model with the lowest DIC, we used this to examine sex differences. We found that the simplest model [total CX/AOTU/POTU~rCBR+sex+(1|Phylogeny)] was performing very close to others, hence used this to make inferences. There were significant sex differences in the CX and the AOTU and none in the

POTU (whole CX: P_{MCMC}=0.026; AOTU: P_{MCMC}=0.004; POTU: P_{MCMC}=0.737), but these sex differences were very small indeed in absolute terms (Figure S1). In absence of any obvious biological inferences we would be able to place on this variation, we continued using sex as a control variable, as to account for variance through sex, only.

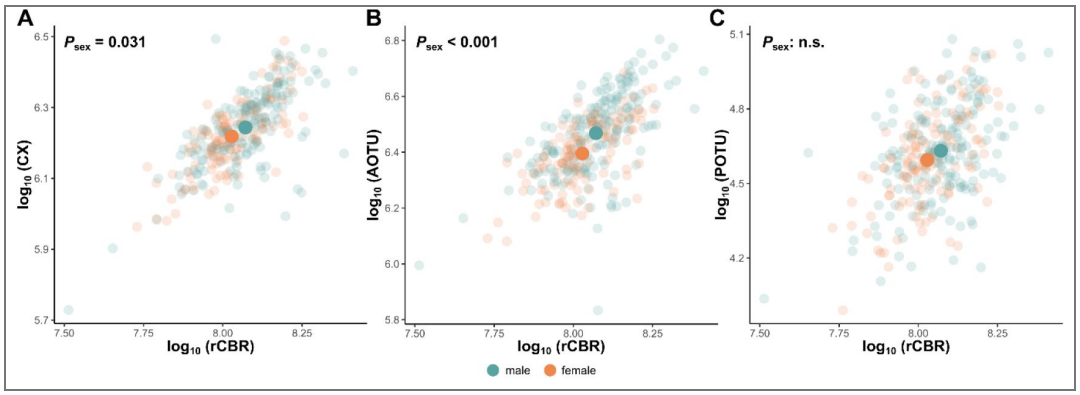

Figure S1. Differences of sex identity onto the relative size of the CX, AOTU and POTU. Significant differences between male and female individuals could be observed in the CX and AOTU (P values of MCMCglmm based models, as [total CX/AOTU/POTU~rCBR+sex+(1|Phylogeny)]). Solid data points indicate sex averages, while opaque circles indicate individual data points. CX central complex, AOTU anterior optic tubercle, POTU posterior optic tubercle, rCBR rest of the central brain.

Figure S2. Central complex neuropils do not show pollen-feeding linked patterns of volumetric expansion A/B:

Assessments of effects of mushroom body size interacting with pollen feeding and with previously identified expansion clades in the CX neuropils, the PB, FB, EB and NO. Shown are test neuropils to rCBR (A) as well as to MB size (B). Results are indicated in each panel; first, the effects of each interaction by assessment of DIC differences, and then the significant relationship between MB and test neuropils. Colour coding was done according to clade differences in mushroom body expansion identified previously. Solid data points indicate species averages, while opaque circles indicate individual data points. Black contours indicate *Heliconius sp*. data points. PB protocerebral bridge, FB fan-shaped body, EB ellipsoid body, NO noduli, MB mushroom bodies, rCBR rest of the central brain. PF pollen feeding.

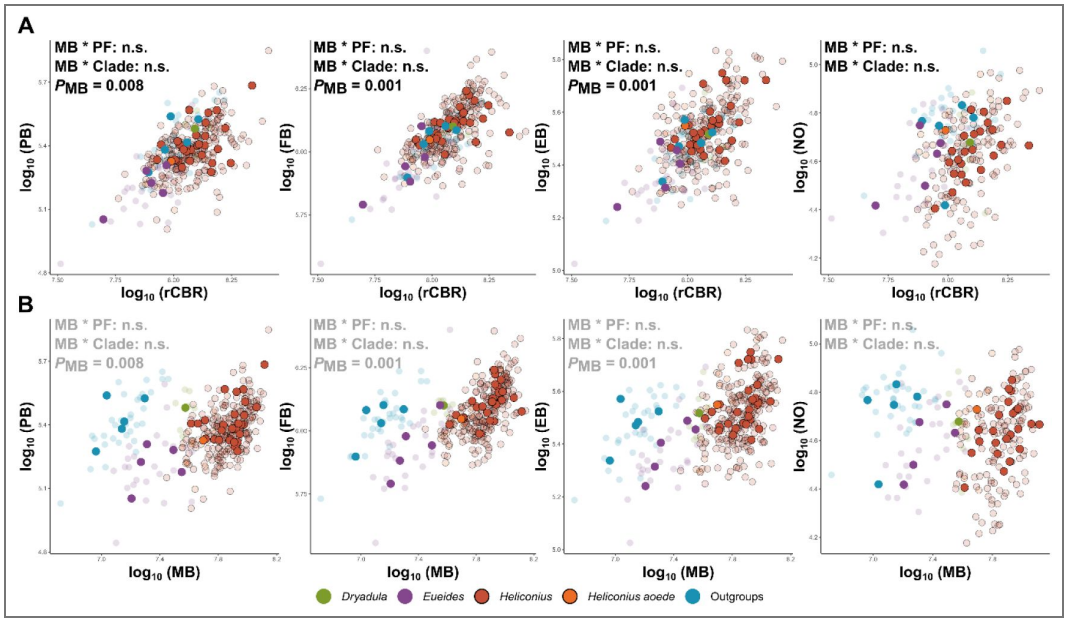

Figure S3. Evolutionary rate analysis in relative CX (A), AOTU (B) and POTU (C) size evolution corroborate an isolated increase of evolutionary rate in the MB concomitant to pollen feeding but not in areas shown here.

Analyses of evolutionary rates of residuals of CX, AOTU and POTU to rCBR regressions. All trees are coloured within their own scale, whereas AOTU and POTU have very similar scale. CX scale is distinct from the one in Figure 2. MB mushroom bodies, CX central complex, AOTU anterior optic tubercle, POTU posterior optic tubercle, rCBR rest of central brain. Pollen feeding picture kindly provided by Sebastian Mena.

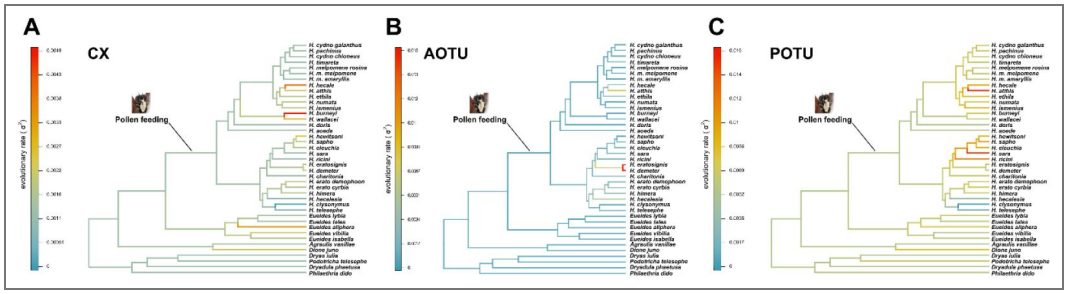

Figure S4. GABA-ergic and serotonergic labelling in additional species A-B:

Labelling of fan-shaped body layer IIIb with Glutamate Decarboxylase (GAD) antibody in *Heliconius erato* and *Euiedes isabella*. **C-D**: Patterns of ramifications in the fan-shaped body of serotonergic neurons labelled through 5-hydroxytryptamine (5-HT) staining. Layers II and III are prominently labelled. Abbreviations: FB fan-shaped body. Scale bars equal 100 µm.

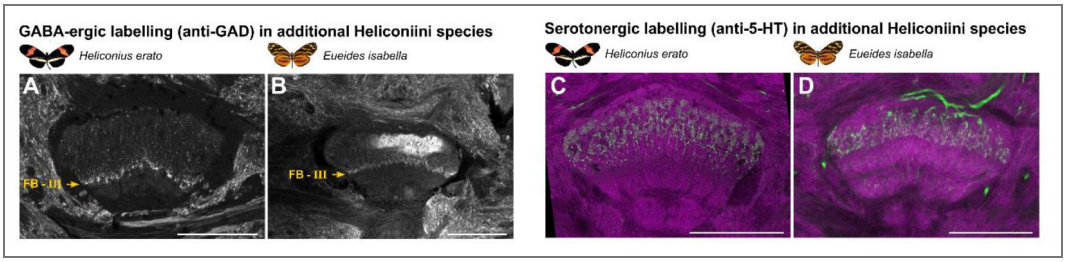

Figure S5. Segmentation of the bulb and its microglomeruli reveals conserved metrics despite increased ER neuron numbers in pollen feeders.

A-B: Location of the ER neuron group and the bulb relative to the brain in *Dryas iulia* (**A**) and *Heliconius melpomene* (**B**). **C-D**: Exemplary confocal images used for subsequent 3D segmentations (green anti-GAD, magenta anti-acetylated tubulin), showing the position of the anterior (1) and posterior (2) portion of the bulb, nestled between the mushroom body lobes dorsally and other parts of the lateral complex ventrally. Arrow indicates the LEa, ultimately ending in the ellipsoid and fan-shaped body.**E-F**: Examples of 3D segmented bulbs. **G-H**: Examples of 3D segmented microglomeruli that were particularly discernible in the posterior portion of the bulb, but otherwise hard to discern. **I-K:** Statistical analyses of bulb volume (points with thick solid strokes), ER neuron numbers (dotted strokes) and an extrapolated number of microglomeruli (no stroke). **I:** To the left in each species are the bulb volume and to the right the number of ER neurons, with no significant difference in bulb size between the two Heliconiini species. **J**: Bulb size in relation to the total number of microglomeruli, which was extrapolated by dividing bulb size with an average microglomerulus size for each individual butterfly. No significant species differences were detected in both variables. **K**: Distribution of the sizes of seven microglomeruli per individual butterfly, with no significant species differences. Abbreviations: ER ellipsoid body ring, BU bulb, MB mushroom bodies. View is anterior, with medial to the right. Scale bars equal 50 µm. See animated 3D segmentations and annotated stacks in file repository.

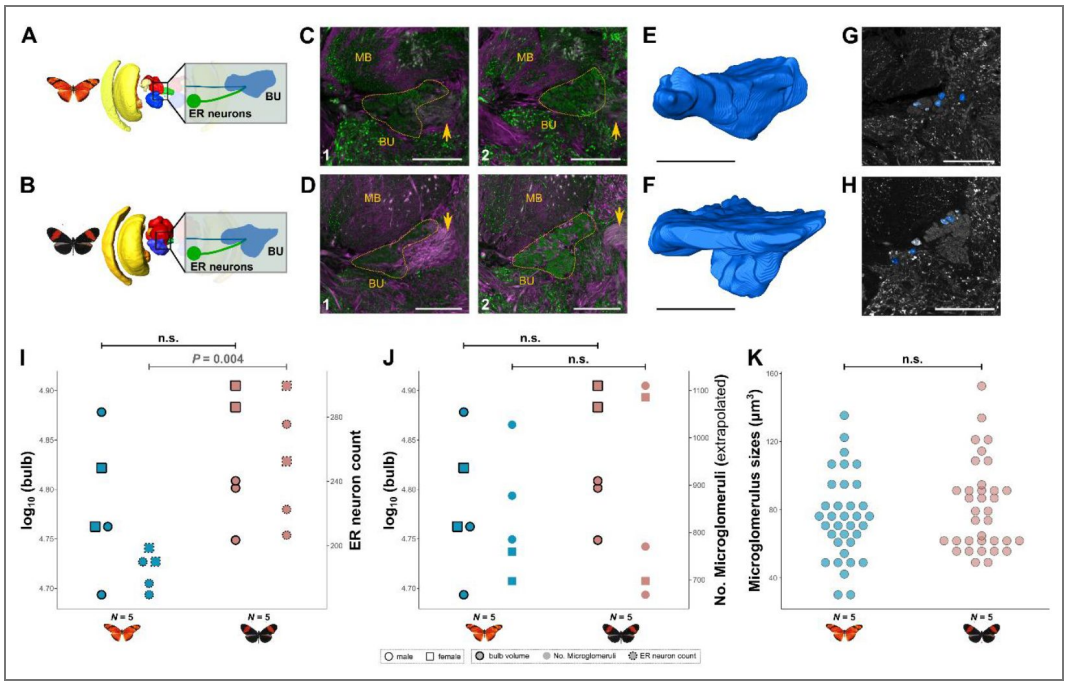

Data availability

Data, R script and readme files associated with this publication is publicly available at *https://doi.org/10.5281/zenodo.15304965*.

Acknowledgements

We thank Antoine Couto for providing the mass injection data in Figure 5, and Francesco Cicconardi for providing image material of the butterfly icons used throughout. We further want to thank Barbara Webb and Stanley Heinze for pointing us to useful computational models in relation to the role of inhibitory ER neurons. We thank Christian Wegener for his insights into the Allatostatin A stainings. This project began under a NERC Independent Research Fellowship NE/N014936/1 and ERC Starter Grant 758508 and was completed under HFSP Project Grant RGP0029/2022 to SHM and BEJ. MSF was supported by a Walter-Benjamin Fellowship from the Deutsche Forschungsgemeinschaft (FA 1818/1-1). YPT is supported by an ERC grant (851040) to Dr Richard M Merrill (LMU), TL is supported by a University of Bristol Scholarship, and EH is supported by an MRC DTP studentship (MR/W006308/1).

Additional information

Author contributions

SHM and MSF conceived the study and formulated the ideas. MSF performed segmentations, stainings and other data acquisitions, performed all statistical analyses and made the figures and the first manuscript draft with input by SHM. YPT and EH segmented AOTU volumes used in the large phylogenetic analysis. TL imaged and segmented the bulbs with input by MSF. BEJ advised on the study and ideas, as well as contributed to interpreting the results and putting them in a wider context. SHM supervised the study and acquired funding.

Funding

Funder	Grant reference number	Author
UKRI | Natural Environment Research Council (NERC)	Independent Research Fellowship NE/N014936/1	Stephen H Montgomery
EC | European Research Council (ERC)	Starter Grant 758508	Stephen H Montgomery
Human Frontier Science Program (HFSP)	Project Grant RGP0029/2022	Basil el Jundi Stephen H Montgomery
Deutsche Forschungsgemeinschaft (DFG)	Walter-Benjamin Fellowship FA 1818/1-1	Max S Farnworth
University of Bristol (bristoluni)	Student Scholarship	Theodora Loupasaki
UKRI | Medical Research Council (MRC)	DTP studentship MR/W006308/1	Theodora Loupasaki Elizabeth A Hodge

Author ORCID iDs

Max S Farnworth: https://orcid.org/0000-0003-2418-3203
Yi Peng Toh: https://orcid.org/0000-0001-7110-5270
Theodora Loupasaki: https://orcid.org/0009-0004-9066-224X
Elizabeth A Hodge: https://orcid.org/0009-0001-1837-4719
Basil el Jundi: https://orcid.org/0000-0002-4539-6681
Stephen H Montgomery: https://orcid.org/0000-0002-5474-5695

Additional files

Figure 4-video 1.
Figure 4-video 2.
Figure 7-video 1.
Figure 7-video 2.
Figure S5-video 1.
Figure S5-video 2.
Table 1.
Table 2.

References

1. **Roberts R. J. V.,** Pop S., Prieto-Godino L. L. (2022) Evolution of central neural circuits: state of the art and perspectives. *Nat Rev Neurosci* **23**:725-743 https://doi.org/10.1038/s41583-022-00644-y | PubMed
2. **Jourjine N.,** Hoekstra H. E. (2021) Expanding evolutionary neuroscience: insights from comparing variation in behavior. *Neuron* **109**:1084-1099 https://doi.org/10.1016/j.neuron.2021.02.002 | PubMed
3. **Farnworth M. S.,** Montgomery S. H. (2024) Evolution of neural circuitry and cognition. *Biology Letters* **20**:20230576 https://doi.org/10.1098/rsbl.2023.0576 | PubMed
4. **Montgomery S. H.,** Mundy N. I., Barton R. A. (2016) Brain evolution and development: adaptation, allometry and constraint. *Proc. R. Soc. B* **283**:20160433 https://doi.org/10.1098/rspb.2016.0433 | PubMed
5. **Tosches M. A.** (2017) Developmental and genetic mechanisms of neural circuit evolution. *Developmental Biology* **431**:16-25 https://doi.org/10.1016/j.ydbio.2017.06.016 | PubMed
6. **Hartenstein V.,** Omoto J. J., Lovick J. K. (2021) The role of cell lineage in the development of neuronal circuitry and function. *Developmental Biology* **475**:165-180 https://doi.org/10.1016/j.ydbio.2020.01.012 | PubMed
7. **Webb B.,** Wystrach A. (2016) Neural mechanisms of insect navigation. *Current Opinion in Insect Science* **15**:27-39 https://doi.org/10.1016/j.cois.2016.02.011 | PubMed
8. **Sun X.,** Yue S., Mangan M. (2020) A decentralised neural model explaining optimal integration of navigational strategies in insects. *eLife* **9**:e54026 https://doi.org/10.7554/eLife.54026 | PubMed
9. **Buehlmann C.,** et al. (2020) Mushroom Bodies Are Required for Learned Visual Navigation, but Not for Innate Visual Behavior, in Ants. *Current Biology* **30**:3438-3443.e2 https://doi.org/10.1016/j.cub.2020.07.013 | PubMed
10. **Collett M.,** Collett T. S. (2018) How does the insect central complex use mushroom body output for steering?. *Current Biology* **28**:R733-R734 https://doi.org/10.1016/j.cub.2018.05.060 | PubMed
11. **Seelig J. D.,** Jayaraman V. (2015) Neural dynamics for landmark orientation and angular path integration. *Nature* **521**:186-191 https://doi.org/10.1038/nature14446 | PubMed
12. **Li F.,** et al. (2020) The connectome of the adult Drosophila mushroom body provides insights into function. *eLife* **9**:e62576 https://doi.org/10.7554/eLife.62576 | PubMed
13. **Lin S.** (2023) The making of the Drosophila mushroom body. *Frontiers in Physiology* **14** https://doi.org/10.3389/fphys.2023.1091248 | PubMed
14. **el Jundi B.,** et al. (2015) Neural coding underlying the cue preference for celestial orientation. *Proceedings of the National Academy of Sciences* **112**:11395-11400 https://doi.org/10.1073/pnas.1501272112 | PubMed

15. **Heinze S.,** Reppert S. M. (2011) Sun Compass Integration of Skylight Cues in Migratory Monarch Butterflies. *Neuron* **69**:345-358 https://doi.org/10.1016/j.neuron.2010.12.025 | PubMed

16. **Nguyen T. A. T.,** Beetz M. J., Merlin C., Pfeiffer K., el Jundi B. (2022) Weighting of Celestial and Terrestrial Cues in the Monarch Butterfly Central Complex. *Front. Neural Circuits* **16** https://doi.org/10.3389/fncir.2022.862279 | PubMed

17. **Stone T.,** et al. (2017) An Anatomically Constrained Model for Path Integration in the Bee Brain. *Current Biology* **27**:3069-3085.e11 https://doi.org/10.1016/j.cub.2017.08.052 | PubMed

18. **Beetz M. J.,** Kraus C., el Jundi B. (2023) Neural representation of goal direction in the monarch butterfly brain. *Nat Commun* **14**:5859 https://doi.org/10.1038/s41467-023-41526-w | PubMed

19. **Mussells Pires P.,** Zhang L., Parache V., Abbott L. F., Maimon G. (2024) Converting an allocentric goal into an egocentric steering signal. *Nature* **626**:808-818 https://doi.org/10.1038/s41586-023-07006-3 | PubMed

20. **Westeinde E. A.,** et al. (2024) Transforming a head direction signal into a goal-oriented steering command. *Nature* **626**:819-826 https://doi.org/10.1038/s41586-024-07039-2 | PubMed

21. **Hulse B. K.,** et al. (2021) A connectome of the Drosophila central complex reveals network motifs suitable for flexible navigation and context-dependent action selection. *eLife* **10**:e66039 https://doi.org/10.7554/eLife.66039 | PubMed

22. **Matheson A. M. M.,** et al. (2022) A neural circuit for wind-guided olfactory navigation. *Nat Commun* **13**:4613 https://doi.org/10.1038/s41467-022-32247-7 | PubMed

23. **Sun X.,** Yue S., Mangan M. (2021) How the insect central complex could coordinate multimodal navigation. *eLife* **10**:e73077 https://doi.org/10.7554/eLife.73077 | PubMed

24. **Ohashi K.,** Thomson J. D. (2009) Trapline foraging by pollinators: its ontogeny, economics and possible consequences for plants. *Ann Bot* **103**:1365-1378 https://doi.org/10.1093/aob/mcp088 | PubMed

25. **Lihoreau M.,** et al. (2013) Unravelling the mechanisms of trapline foraging in bees. *Communicative & Integrative Biology* **6**:e22701 https://doi.org/10.4161/cib.22701 | PubMed

26. **Kuwabara T.,** Kohno H., Hatakeyama M., Kubo T. (2023) Evolutionary dynamics of mushroom body Kenyon cell types in hymenopteran brains from multifunctional type to functionally specialized types. *Science Advances* **9**:eadd4201 https://doi.org/10.1126/sciadv.add4201 | PubMed

27. **Farris S. M.** (2013) Evolution of Complex Higher Brain Centers and Behaviors: Behavioral Correlates of Mushroom Body Elaboration in Insects. *Bbe* **82**:9-18 https://doi.org/10.1159/000352057 | PubMed

28. **Farnworth M. S.,** Loupasaki T., Couto A., Montgomery S. H. (2024) Mosaic evolution of a learning and memory circuit in Heliconiini butterflies. *Current Biology* **34**:5252-5262.e5 https://doi.org/10.1016/j.cub.2024.09.069 | PubMed

29. **Couto A.,** et al. (2023) Rapid expansion and visual specialisation of learning and memory centres in the brains of Heliconiini butterflies. *Nat Commun* **14**:4024 https://doi.org/10.1038/s41467-023-39618-8 | PubMed

30. **Farris S. M.,** Schulmeister S. (2011) Parasitoidism, not sociality, is associated with the evolution of elaborate mushroom bodies in the brains of hymenopteran insects. *Proceedings of the Royal Society B: Biological Sciences* **278**:940-951 https://doi.org/10.1098/rspb.2010.2161 | PubMed

31. **Honkanen A.,** Adden A., Freitas J., da S., Heinze S. (2019) The insect central complex and the neural basis of navigational strategies. *Journal of Experimental Biology* **222**:jeb188854 https://doi.org/10.1242/jeb.188854 | PubMed

32. **Young F. J.,** Montgomery S. H. (2020) Pollen feeding in Heliconius butterflies: the singular evolution of an adaptive suite. *Proceedings of the Royal Society B: Biological Sciences* **287**:20201304 https://doi.org/10.1098/rspb.2020.1304 | PubMed

33. **Sayre M. E.,** Templin R., Chavez J., Kempenaers J., Heinze S. (2021) A projectome of the bumblebee central complex. *eLife* **10**:e68911 https://doi.org/10.7554/eLife.68911 | PubMed

34. **Moura P. A.,** Corso G., Montgomery S. H., Cardoso M. Z. (2022) True site fidelity in pollen-feeding butterflies. *Functional Ecology* **36**:572-582 https://doi.org/10.1111/1365-2435.13976

35. **Moura P. A.,** Cardoso M. Z., Montgomery S. H. (2024) Heliconius butterflies use wide-field landscape features, but not individual local landmarks, during spatial learning. *Royal Society Open Science* **11**:241097 https://doi.org/10.1098/rsos.241097 | PubMed

36. **Young F. J.,** et al. (2024) Enhanced long-term memory and increased mushroom body plasticity in Heliconius butterflies. *iScience* **27**:108949 https://doi.org/10.1016/j.isci.2024.108949 | PubMed

37. **Hodge E. A.,** et al. (2025) Modality-specific long-term memory enhancement in Heliconius butterflies. *Philos Trans R Soc Lond B Biol Sci* **380**:20240119 https://doi.org/10.1098/rstb.2024.0119 | PubMed

38. **Doussot C.,** Purdy J., Lihoreau M. (2024) Chapter 4 - Navigation: Cognition, learning, and memory. In: Purdy J. (Ed). *The Foraging Behavior of the Honey Bee (Apis mellifera, L.)* Academic Press. pp. 85-104 https://doi.org/10.1016/B978-0-323-91793-3.00007-9

39. **Collett T. S.,** Collett M. (2002) Memory use in insect visual navigation. *Nat Rev Neurosci* **3**:542-552 https://doi.org/10.1038/nrn872 | PubMed

40. **Collett M.,** Chittka L., Collett T. S. (2013) Spatial Memory in Insect Navigation. *Current Biology* **23**:R789-R800 https://doi.org/10.1016/j.cub.2013.07.020 | PubMed

41. **Moura P. A.,** Young F. J., Monllor M., Cardoso M. Z., Montgomery S. H. (2023) Long-term spatial memory across large spatial scales in Heliconius butterflies. *Current Biology* **33**:R797-R798 https://doi.org/10.1016/j.cub.2023.06.009 | PubMed

42. **Brown K. S. x** (1981) The Biology of Heliconius and Related Genera. *Annual Review of Entomology* **26**:427-457 https://doi.org/10.1146/annurev.en.26.010181.002235

43. **Hebberecht L.,** Melo-Flórez L., Young F. J., McMillan W. O., Montgomery S. H. (2022) The evolution of adult pollen feeding did not alter postembryonic growth in Heliconius butterflies. *Ecology and Evolution* **12**:e8999 https://doi.org/10.1002/ece3.8999 | PubMed

44. **Hodge E. A.,** et al. (2026) Conservation of sensory pathways implies a localised change in the mushroom bodies is associated with cognitive evolution in Heliconius butterflies. *Evol qpag005* **80**:765-778 https://doi.org/10.1093/evolut/qpag005 | PubMed

45. **Kandimalla P.,** Omoto J. J., Hong E. J., Hartenstein V. (2023) Lineages to circuits: the developmental and evolutionary architecture of information channels into the central complex. *J Comp Physiol A* **209**:679-720 https://doi.org/10.1007/s00359-023-01616-y | PubMed

46. **Homberg U.,** et al. (2023) The sky compass network in the brain of the desert locust. *J Comp Physiol A* **209**:641-662 https://doi.org/10.1007/s00359-022-01601-x | PubMed

47. **Heinze S.,** Reppert S. M. (2012) Anatomical basis of sun compass navigation I: The general layout of the monarch butterfly brain. *Journal of Comparative Neurology* **520**:1599-1628 https://doi.org/10.1002/cne.23054 | PubMed

48. **Beetz M. J.,** el Jundi B., Heinze S., Homberg U. (2015) Topographic organization and possible function of the posterior optic tubercles in the brain of the desert locust Schistocerca gregaria. *Journal of Comparative Neurology* **523**:1589-1607 https://doi.org/10.1002/cne.23736 | PubMed

49. **Jundi B.,** Homberg U. (2010) Evidence for the possible existence of a second polarization-vision pathway in the locust brain. *Journal of Insect Physiology* **56**:971-979 https://doi.org/10.1016/j.jinsphys.2010.05.011 | PubMed

50. **Heinze S.,** Homberg U. (2007) Maplike Representation of Celestial E-Vector Orientations in the Brain of an Insect. *Science* **315**:995-997 https://doi.org/10.1126/science.1135531 | PubMed

51. **von Hadeln J.,** et al. (2020) Neuroarchitecture of the central complex of the desert locust: Tangential neurons. *Journal of Comparative Neurology* **528**:906-934 https://doi.org/10.1002/cne.24796 | PubMed

52. **Jahn S.,** et al. (2023) Neuroarchitecture of the central complex in the Madeira cockroach Rhyparobia maderae: Pontine and columnar neuronal cell types. *Journal of Comparative Neurology* **531**:1689-1714 https://doi.org/10.1002/cne.25535 | PubMed

53. **Heinze S.,** Homberg U. (2008) Neuroarchitecture of the central complex of the desert locust: Intrinsic and columnar neurons. *Journal of Comparative Neurology* **511**:454-478 https://doi.org/10.1002/cne.21842 | PubMed

54. **Pfeiffer K.** (2023) The neuronal building blocks of the navigational toolkit in the central complex of insects. *Current Opinion in Insect Science* **55**:100972 https://doi.org/10.1016/j.cois.2022.100972 | PubMed

55. **Heinze S.** (2024) Variations on an ancient theme — the central complex across insects. *Current Opinion in Behavioral Sciences* **57**:101390 https://doi.org/10.1016/j.cobeha.2024.101390

56. **Jan L. Y.,** Jan Y. N. (1982) Antibodies to horseradish peroxidase as specific neuronal markers in Drosophila and in grasshopper embryos. *Proceedings of the National Academy of Sciences* **79**:2700-2704 https://doi.org/10.1073/pnas.79.8.2700 | PubMed

57. **Heinze S.,** Florman J., Asokaraj S., Jundi B. el, Reppert S. M. (2013) Anatomical basis of sun compass navigation II: The neuronal composition of the central complex of the monarch butterfly. *Journal of Comparative Neurology* **521**:267-298 https://doi.org/10.1002/cne.23214 | PubMed

58. **Farnworth M. S.,** Bucher G., Hartenstein V. (2022) An atlas of the developing Tribolium castaneum brain reveals conservation in anatomy and divergence in timing to Drosophila melanogaster. *Journal of Comparative Neurology* **530**:2335-2371 https://doi.org/10.1002/cne.25335 | PubMed

59. **Farnworth M. S.,** Eckermann K. N., Bucher G. (2020) Sequence heterochrony led to a gain of functionality in an immature stage of the central complex: A fly–beetle insight. *PLOS Biology* **18**:e3000881 https://doi.org/10.1371/journal.pbio.3000881 | PubMed

60. **Timm J.,** Scherner M., Matschke J., Kern M., Homberg U. (2021) Tyrosine hydroxylase immunostaining in the central complex of dicondylian insects. *Journal of Comparative Neurology* **529**:3131-3154 https://doi.org/10.1002/cne.25151 | PubMed

61. **Homberg U.,** et al. (2023) Comparative morphology of serotonin-immunoreactive neurons innervating the central complex in the brain of dicondylian insects. *J Comp Neurol* **531**:1482-1508 https://doi.org/10.1002/cne.25529 | PubMed

62. **Crittenden J. R.,** Skoulakis E. M. C., Han K.-A., Kalderon D., Davis R. L. (1998) Tripartite Mushroom Body Architecture Revealed by Antigenic Markers. *Learn Mem* **5**:38-51 https://doi.org/10.1101/lm.5.1.38 | PubMed

63. **Ito K.,** et al. (2014) A Systematic Nomenclature for the Insect Brain. *Neuron* **81**:755-765 https://doi.org/10.1016/j.neuron.2013.12.017 | PubMed

64. **Wolff T.,** Iyer N. A., Rubin G. M. (2015) Neuroarchitecture and neuroanatomy of the Drosophila central complex: A GAL4-based dissection of protocerebral bridge neurons and circuits. *Journal of Comparative Neurology* **523**:997-1037 https://doi.org/10.1002/cne.23705 | PubMed

65. **Jundi B. el,** Baird E., Byrne M. J., Dacke M. (2019) The brain behind straight-line orientation in dung beetles. *Journal of Experimental Biology* **222**:jeb192450 https://doi.org/10.1242/jeb.192450 | PubMed

66. **Homberg U.,** Humberg T.-H., Seyfarth J., Bode K., Pérez M. Q. (2018) GABA immunostaining in the central complex of dicondylian insects. *Journal of Comparative Neurology* **526**:2301-2318 https://doi.org/10.1002/cne.24497 | PubMed

67. **Yang J. S.,** et al. (2013) Diverse neuronal lineages make stereotyped contributions to the Drosophila locomotor control center, the central complex. *Journal of Comparative Neurology* **521**:2645-2662 https://doi.org/10.1002/cne.23339 | PubMed

68. **Omoto J. J.,** et al. (2017) Visual Input to the Drosophila Central Complex by Developmentally and Functionally Distinct Neuronal Populations. *Current Biology* **27**:1098-1110 https://doi.org/10.1016/j.cub.2017.02.063 | PubMed

69. **Kahsai L.,** Winther Å.M.E. (2011) Chemical neuroanatomy of the Drosophila central complex: Distribution of multiple neuropeptides in relation to neurotransmitters. *Journal of Comparative Neurology* **519**:290-315 https://doi.org/10.1002/cne.22520 | PubMed

70. **Nässel D. R.,** Homberg U. (2006) Neuropeptides in interneurons of the insect brain. *Cell Tissue Res* **326**:1-24 https://doi.org/10.1007/s00441-006-0210-8 | PubMed

71. **Vitzthum H.,** Homberg U., Agricola H. (1996) Distribution of Dip-allatostatin I-like immunoreactivity in the brain of the locust Schistocerca gregaria with detailed analysis of immunostaining in the central complex. *Journal of Comparative Neurology* **369**:419-437 https://doi.org/10.1002/(sici)1096-9861(19960603)369:3<419::aid-cne7>3.0.co;2-8 | PubMed

72. **Pfeiffer K.,** Homberg U. (2014) Organization and Functional Roles of the Central Complex in the Insect Brain. *Annual Review of Entomology* **59**:165-184 https://doi.org/10.1146/annurev-ento-011613-162031 | PubMed

73. **Wegener C.,** Chen J. (2022) Allatostatin A Signalling: Progress and New Challenges From a Paradigmatic Pleiotropic Invertebrate Neuropeptide Family. *Front. Physiol* **13** https://doi.org/10.3389/fphys.2022.920529 | PubMed

74. **Schoofs L.,** Loof A. D., Hiel M. B. V. (2017) Neuropeptides as Regulators of Behavior in Insects. *Annual Review of Entomology* **62**:35-52 https://doi.org/10.1146/annurev-ento-031616-035500 | PubMed

75. **Kaiser A.,** et al. (2022) A three-dimensional atlas of the honeybee central complex, associated neuropils and peptidergic layers of the central body. *Journal of Comparative Neurology* **530**:2416-2438 https://doi.org/10.1002/cne.25339 | PubMed

76. **Konstantinides N.,** Desplan C. (2024) Neuronal Circuit Evolution: From Development to Structure and Adaptive Significance. *Cold Spring Harb Perspect Biol* **17**:a041493 https://doi.org/10.1101/cshperspect.a041493 | PubMed

77. **Logan C. J.,** et al. (2018) Beyond brain size: Uncovering the neural correlates of behavioral and cognitive specialization. *Comparative Cognition and Behavior Reviews* **13**:55-90 https://doi.org/10.3819/CCBR.2018.130008

78. **Chittka L.,** Niven J. (2009) Are Bigger Brains Better?. *Current Biology* **19**:R995-R1008 https://doi.org/10.1016/j.cub.2009.08.023 | PubMed

79. **el Jundi B.,** Warrant E. J., Pfeiffer K., Dacke M. (2018) Neuroarchitecture of the dung beetle central complex. *Journal of Comparative Neurology* **0** https://doi.org/10.1002/cne.24520 | PubMed

80. **Hensgen R.,** England L., Homberg U., Pfeiffer K. (2021) Neuroarchitecture of the central complex in the brain of the honeybee: Neuronal cell types. *Journal of Comparative Neurology* **529**:159-186 https://doi.org/10.1002/cne.24941 | PubMed

81. **Hulse B. K.,** Jayaraman V. (2020) Mechanisms Underlying the Neural Computation of Head Direction. *Annual Review of Neuroscience* **43**:31-54 https://doi.org/10.1146/annurev-neuro-072116-031516 | PubMed

82. **Nguyen T. A. T.,** Beetz M. J., Merlin C., el Jundi B. (2021) Sun compass neurons are tuned to migratory orientation in monarch butterflies. *Proceedings of the Royal Society B: Biological Sciences* **288**:20202988 https://doi.org/10.1098/rspb.2020.2988 | PubMed

83. **Pisokas I.,** Heinze S., Webb B. (2020) The head direction circuit of two insect species. *eLife* **9**:e53985 https://doi.org/10.7554/eLife.53985 | PubMed

84. **Giraldo Y. M.,** et al. (2018) Sun Navigation Requires Compass Neurons in Drosophila. *Current Biology* **28**:2845-2852.e4 https://doi.org/10.1016/j.cub.2018.07.002 | PubMed

85. **Walsh K. T.,** Doe C. Q. (2017) Drosophila embryonic type II neuroblasts: origin, temporal patterning, and contribution to the adult central complex. *Development* **144**:4552-4562 https://doi.org/10.1242/dev.157826 | PubMed

86. **Andrade I. V.,** et al. (2019) Developmentally Arrested Precursors of Pontine Neurons Establish an Embryonic Blueprint of the Drosophila Central Complex. *Current Biology* **29**:412-425.e3 https://doi.org/10.1016/j.cub.2018.12.012 | PubMed

87. **Lyu C.,** Abbott L. F., Maimon G. (2022) Building an allocentric travelling direction signal via vector computation. *Nature* **601**:92-97 https://doi.org/10.1038/s41586-021-04067-0 | PubMed

88. **Lu J.,** et al. (2022) Transforming representations of movement from body-to world-centric space. *Nature* **601**:98-104 https://doi.org/10.1038/s41586-021-04191-x | PubMed

89. **Donlea J. M.,** et al. (2018) Recurrent Circuitry for Balancing Sleep Need and Sleep. *Neuron* **97**:378-389.e4 https://doi.org/10.1016/j.neuron.2017.12.016 | PubMed

90. **Mota T.,** et al. (2016) Synaptic Organization of Microglomerular Clusters in the Lateral and Medial Bulbs of the Honeybee Brain. *Front. Neuroanat* **10** https://doi.org/10.3389/fnana.2016.00103 | PubMed

91. **Held M.,** et al. (2016) Microglomerular Synaptic Complexes in the Sky-Compass Network of the Honeybee Connect Parallel Pathways from the Anterior Optic Tubercle to the Central Complex. *Front. Behav. Neurosci* **10** https://doi.org/10.3389/fnbeh.2016.00186 | PubMed

92. **Schmitt F.,** Stieb S. M., Wehner R., Rössler W. (2016) Experience-related reorganization of giant synapses in the lateral complex: Potential role in plasticity of the sky-compass pathway in the desert ant Cataglyphis fortis. *Developmental Neurobiology* **76**:390-404 https://doi.org/10.1002/dneu.22322 | PubMed

93. **Träger U.,** Wagner R., Bausenwein B., Homberg U. (2008) A novel type of microglomerular synaptic complex in the polarization vision pathway of the locust brain. *Journal of Comparative Neurology* **506**:288-300 https://doi.org/10.1002/cne.21512 | PubMed

94. **Le Moël F.,** Stone T., Lihoreau M., Wystrach A., Webb B. (2019) The Central Complex as a Potential Substrate for Vector Based Navigation. *Front. Psychol* **10** https://doi.org/10.3389/fpsyg.2019.00690 | PubMed

95. **Finkbeiner S. D.** (2014) Communal Roosting in Heliconius Butterflies (Nymphalidae): Roost Recruitment, Establishment, Fidelity, and Resource Use Trends Based on Age and Sex. *lepi* **68**:10-16 https://doi.org/10.18473/lepi.v68i1.a2

96. **Kreissl S.,** Strasser C., Galizia C. G. (2010) Allatostatin immunoreactivity in the honeybee brain. *Journal of Comparative Neurology* **518**:1391-1417 https://doi.org/10.1002/cne.22343 | PubMed

97. **Urlacher E.,** et al. (2016) Honey Bee Allatostatins Target Galanin/Somatostatin-Like Receptors and Modulate Learning: A Conserved Function?. *PLOS One* **11**:e0146248 https://doi.org/10.1371/journal.pone.0146248 | PubMed

98. **Yamagata N.,** Hiroi M., Kondo S., Abe A., Tanimoto H. (2016) Suppression of Dopamine Neurons Mediates Reward. *PLOS Biology* **14**:e1002586 https://doi.org/10.1371/journal.pbio.1002586 | PubMed

99. **Suárez-Grimalt R.,** Raccuglia D. (2021) The neural architecture of sleep regulation – insights from Drosophila. *Neuroforum* **27**:189-199 https://doi.org/10.1515/nf-2021-0018

100. **Fisher Y. E.,** Lu J., D'Alessandro I., Wilson R. I. (2019) Sensorimotor experience remaps visual input to a heading-direction network. *Nature* **576**:121-125 https://doi.org/10.1038/s41586-019-1772-4 | PubMed

101. **Collett T.,** Graham P., Heinze S. (2025) The neuroethology of ant navigation. *Current Biology* **35**:R110-R124 https://doi.org/10.1016/j.cub.2024.12.034 | PubMed

102. **Montgomery S. H.,** Merrill R. M., Ott S. R. (2016) Brain composition in Heliconius butterflies, posteclosion growth and experience-dependent neuropil plasticity. *Journal of Comparative Neurology* **524**:1747-1769 https://doi.org/10.1002/cne.23993 | PubMed

103. **team Posit** (2023) *RStudio: Integrated Development Environment for R* Posit Software, PBC, Boston, MA.

104. **R Core Team** (2023) *R: A Language and Environment for Statistical Computing* Vienna, Austria: R Foundation for Statistical Computing.

105. **Hadfield J. D.** (2010) MCMC Methods for Multi-Response Generalized Linear Mixed Models: The MCMCglmm R Package. *Journal of Statistical Software* **33**:1-22 https://doi.org/10.18637/jss.v033.i02

106. **Ott S. R.** (2008) Confocal microscopy in large insect brains: Zinc–formaldehyde fixation improves synapsin immunostaining and preservation of morphology in whole-mounts. *Journal of Neuroscience Methods* **172**:220-230 https://doi.org/10.1016/j.jneumeth.2008.04.031 | PubMed

107. **Bucher D.,** Scholz M., Stetter M., Obermayer K., Pflüger H.-J. (2000) Correction methods for three-dimensional reconstructions from confocal images: I. tissue shrinking and axial scaling. *Journal of Neuroscience Methods* **100**:135-143 https://doi.org/10.1016/s0165-0270(00)00245-4 | PubMed

108. **Schindelin J.,** et al. (2012) Fiji: an open-source platform for biological-image analysis. *Nat Methods* **9**:676-682 https://doi.org/10.1038/nmeth.2019 | PubMed

109. **Cicconardi F.,** et al. (2023) Evolutionary dynamics of genome size and content during the adaptive radiation of Heliconiini butterflies. *Nat Commun* **14**:5620 https://doi.org/10.1038/s41467-023-41412-5 | PubMed

Farnworth MS (2026) Dataset VS2 associated with publication of Farnworth et al "Distinct evolutionary trajectories of two integration centres, the central complex and mushroom bodies, across Heliconiini butterflies". Zenodo. https://doi.org/10.5281/zenodo.15304965

Couto A, Young F, Atzeni D, Marty S, Melo-Flórez L, Hebberecht L, Monllor M, Neal C, Cicconardi F, McMillan W, *et al.* (2023) Data From: Rapid expansion and visual specialisation of learning and memory centers in the brains of Heliconiini butterflies. Dryad Digital Repository. https://doi.org/10.5061/dryad.f1vhhmh28

Peer reviews

Reviewer #1 (Public review):

The authors previously reported that Heliconius, one genus of the Heliconiini butterflies, evolved to be efficient foragers to feed pollen of specific plants and have massively expanded mushroom bodies. Using the same image dataset, the authors segmented the central complex and associated brain regions and found that the volume of the central complex relative to the rest of brain are largely conserved across the Heliconiini butterflies. By performing immunostaining to label specific subset of neurons, the authors found several potential sites of evolutional divergence in the central complex neural circuits, including the numbers of GABAergic ellipsoid body ring neurons and the innervation patterns of Allatostatin A expressing neurons in the noduli. These neuroanatomical data will be helpful to guide the future studies to understand the evolution of the neural circuits for vector-based navigations.

Strength

The authors used sufficiently large scale of dataset from 307 individuals of 41 specifies of Heliconiini butterflies to solidify the quantitative conclusions, and present new microscopy data for fine neuroanatomical comparison of the central complex.

Weakness

(1) Although the figures display a concise summary of anatomical findings, it would be difficult for non-experts to learn from this manuscript to identify the same neuronal processes in the raw confocal stacks. It would be helpful to have instructive movies to show step by step guide for identifications of neurons of interests, segmentations and 3D visualizations (rotation) for several examples including ER neurons (to supplement texts in line 347-353) and Allatostatin A neurons.

(2) Related to (1), it was difficult for me to access if the data in Fig 7 support the author's conclusions that ER neuron number increased in Heliconius Melpomene. By my understanding, the resolution of this dataset isn't high enough to trace individual axons and therefore authors do not rule out that the portion of "ER ring neurons" in Heliconius may not innervate the ER, as stated in Line 635 "Importantly, we also found that some ER neurons

bypass the ellipsoid body and give rise to dense branches within distinct layers in the fan-shaped body (ER-FB)". If they don't innervate the ellipsoid body, why are they named as "ER neurons"?

(3) Discussions around the line 577-584 requires the assumption that each ellipsoid body (EB) ring neuron typically arborise in a single microglomerulus to form largely one-to-one connection with TuBu neurons within the bulb (BU), and therefore the number of BU microglomeruli should provide an estimation of the number of ER neurons. Explain this key assumption or provide an alternative explanation.

(4) The details of antibody information are missing in the Key resource table. Instead of citing papers, list the catalogue numbers and identifier for commercially available antibodies, and describe the antigen and if they are monoclonal or polyclonal. Are antigens conserved across species?

(5) I did not understand why authors assume that foraging to feed on pollens is more difficult cognitive task than foraging to feed on nectars. Would it be possible that they are equality demanding tasks but pollen feeding allows Heliconius to pass more proteins and nucleic acids to their offsprings and therefore they can develop larger mushroom bodies?

Comments on revisions:

The authors fully addressed my concerns and significantly improved the accessibility of the manuscript.

https://doi.org/10.7554/eLife.107589.2.sa2

Reviewer #2 (Public review):

Summary

In this study, Farnsworth et al. ask whether the previously established expansion of mushroom bodies in the pollen foraging Heliconius genus of Heliconiini butterflies co-evolved with adaptations in the central complex. Heliconius trap line foraging strategies to acquire pollen as a novel resource require advanced spatial memory mediated by larger mushroom bodies but the authors show that related navigation circuits in the central complex are highly conserved across the Heliconiini tribe, with a few interesting exceptions. Using general immunohistochemical stains and 3D reconstruction, the authors compared volumes of central complex regions and unlike the mushroom bodies, there was no evidence of expansion associated with pollen feeding. However, a second dataset of neuromodulator and neuropeptide antibody labeling reveal more subtle differences between pollen and non-pollen foragers and highlight sub-circuits that may mediate species-specific differences in behavior. Specifically, the authors found an expansion of GABAergic ER neurons projecting to the fan shaped body in Heliconius which may enhance their ability to path-integrate. They also found differences in Allatostatin A immunoreactivity, particularly increased expression in the noduli associated with pollen feeding. These differences warrant closer examination in future studies to determine their functional implication on navigation and foraging behaviors.

Strengths

The authors leveraged a large morphological data set from the Heliconiini to achieve excellent phylogenetic coverage across the tribe with 41 species represented. Their high quality histology resolves anatomical details to the level of specific, identifiable tracts and cell body clusters. They revealed differences at a circuit level, which would not be obvious from a volumetric comparison. The discussion of these adaptations in the context of central complex

models is useful for generating new hypotheses for future studies on the function of ER-FB neurons and the role of Allatostatin A modulation in navigation.

The conclusions drawn in this paper are measured and supported by rigorous statistics and evidence from micrographs.

Weaknesses

The majority of results in this study do not reveal adaptations in the central complex associated with pollen foraging. However, reporting conserved traits is useful and illustrates where developmental or functional constraints may be acting. The authors have now revised the introduction to set up two alternate hypotheses..

In the main text, the authors describe differences in GABAergic ER neurons between H. melpomene and an outgroup species, with additional images from other species in Figure S4. Quantification of ER cells in these other species would strengthen the claim that these are increased in Heliconius and not just the focal species, but this may hopefully be pursued in future studies.

Comments on revisions:

I am satisfied with the authors' revisions.

https://doi.org/10.7554/eLife.107589.2.sa1

Author response:

The following is the authors' response to the original reviews.

> ***eLife Assessment***
>
> *The analysis of neural morphology across Heliconiini butterfly species revealed brain area specific changes associated with new foraging behaviours. While the volume of the centre for learning and memory, the mushroom bodies, was known to vary widely across species, new, valuable results show conservation of the volume of a center for navigation, the central complex. The presented evidence is convincing for both volumetric conservation in the central complex and fine neuroanatomical differences associated with pollen feeding, delivered by experimental approaches that are applicable to other insect species. This work will be of interest to evolutionary biologists, entomologists, and neuroscientists.*

Many thanks for your assessment and time handling this manuscript. We value the constructive input of both reviewers and believe that the result is an improved publication.

> ***Public Reviews:***
>
> ***Reviewer #1 (Public review):***
>
> *The authors previously reported that Heliconius, one genus of the Heliconiini butterflies, evolved to be efficient foragers to feed pollen of specific plants and have massively expanded mushroom bodies. Using the same image dataset, the authors segmented the central complex and associated brain regions and found that the volume of the central complex relative to the rest of the brain is largely conserved across the Heliconiini butterflies. By performing immunostaining to label a specific subset of neurons, the authors found several potential sites of evolutionary divergence in the central complex neural circuits, including the number of GABAergic ellipsoid body ring neurons and the innervation patterns of Allatostatin A expressing neurons in the noduli. These*

> *neuroanatomical data will be helpful to guide future studies to understand the evolution of the neural circuits for vector-based navigation.*

We thank Reviewer 1 for the constructive feedback and criticism, which will have strengthened this publication.

> *Strengths:*
>
> *The authors used a sufficiently large scale of dataset from 307 individuals of 41 species of Heliconiini butterflies to solidify the quantitative conclusions and present new microscopy data for fine neuroanatomical comparison of the central complex.*
>
> *Weaknesses:*
>
> *(1) Although the figures display a concise summary of anatomical findings, it would be difficult for non-experts to learn from this manuscript to identify the same neuronal processes in the raw confocal stacks. It would be helpful to have instructive movies to show a step-by-step guide for identification of neurons of interest, segmentations, and 3D visualizations (rotation) for several examples, including ER neurons (to supplement texts in line 347-353) and Allatostatin A neurons.*

We approached this with the following logic:

All 3D segmentations were animated, to illustrate how they are generated from raw imaging data. This means we are providing a video file for each major species group (*Heliconius*/outgroup-Heliconiini) for Figure 4 (general CX anatomy), Figure 7 (ER neuron projections), Figure S5 (ER neuron/bulb anatomy). This visual connection should help the reader relate 3D segmentations to image stacks. We have also added a reference to these videos in the relevant Figure captions.

We also annotated image stacks, but did so selectively. We annotated key stacks of Figure 4 (general CX anatomy), Figure 7 (ER neuron projections), Figure S5 (ER neuron/bulb anatomy) and include a reference in figure caption to them.

We refrained from annotating stacks of Figures 5, 6, 8 and S4. This is because we believe that the annotations we have performed in the figure panels will be sufficient for readers interested in the finer detail of these anatomies who are familiar with general CX anatomy.

We believe that our approach will help the reader to gain a visual illustration of those parts of the manuscript which report key results and novel insights, such as ER neuronal variation, and that the data and figures collectively provide accessible information sufficient for this purpose.

Text changes in Figure captions 4, 7 and S5: “See animated 3D segmentations and annotated stacks in file repository.”

> *(2) Related to (1), it was difficult for me to assess if the data in Figure 7 support the author's conclusions that ER neuron number increased in Heliconius Melpomene. By my understanding, the resolution of this dataset isn't high enough to trace individual axons and therefore authors do not rule out that the portion of "ER ring neurons" in Heliconius may not innervate the ER, as stated in Line 635 "Importantly, we also found that some ER neurons bypass the ellipsoid body and give rise to dense branches within distinct layers in the fan-shaped body (ER-FB)". If they don't innervate the ellipsoid body, why are they named as "ER neurons"?*

Thanks for pointing to this. We believe this is primarily a nomenclature issue but have tried to specify in the text.

Ultimately, neurons from this group that project to the EB forming the actual ring neurons and those that project to the FB with unclear function, thus far, emerge through the same lineage, DALv2 (as determined by Kandimalla et al 2023) and therefore have common developmental origin (also noted by Homberg et al 2018). To acknowledge their common developmental origin and to simplify nomenclature, and therefore also provide easier comprehension by non-experts, we specify which DALv2 progeny project to which areas, but refer to both adult neuron populations to "ER neurons". We have changed the following text to acknowledge our definition specifically, which we hope mitigates the understandable confusion.

Lines 354-357: "Here, we refer to these neurons, as well as those neurons projecting to the fan-shaped body (GU neurons in [66]), as ER neurons due to their common developmental origin [45,66] and to simplify anatomical descriptions."

Lines 386-387: "Whether these ER neurons solely branch in the fan-shaped body, as shown for GU neurons elsewhere [66] or have additional side branches entering the ellipsoid body is not clear."

> *(3) Discussions around the lines 577-584 require the assumption that each ellipsoid body (EB) ring neuron typically arborises in a single microglomerulus to form a largely one-to-one connection with TuBu neurons within the bulb (BU), and therefore, the number of BU microglomeruli should provide an estimation of the number of ER neurons. Explain this key assumption or provide an alternative explanation.*

Thanks for this. We do not think that our hypothesis necessarily requires any specific assumptions regarding the ratio of microglomerulus to ER or TuBu neurons. Even in *Drosophila* the ratio of ER to MG is only approximately 1:1, as some microglomeruli seem to combine into one. In other species this relationship might be very different. Indeed, our data suggests that in outgroup-Heliconiini the ratio is 4.4 microglomeruli to 1 ER neuron, and in *Heliconius* it is 3.4. However, as these MG numbers are extrapolated and cannot be precisely counted, they may be too imprecise to come to a definite conclusion, hence why we do not mention this in the text. Importantly, extrapolation in the current form is a valid additional way for us to describe overall bulb anatomy (next to bulb volume, average microglomerulus size).

In any case, the inference we make here is that a conserved bulb anatomy in volume, MG numbers and size supports our assumption that the additional neurons in the ER neuron group/DALv2 progeny do not arborize in the bulb, but do so in the SMP/SLP region and in the fanshaped body. We believe we have described this inference accurately in the current manuscript.

An additional point, not mentioned in the manuscript, but emerging through lineage annotations of connectome data, is that some DALv2 progeny have been identified as MBONs as well as being GABA-ergic, which could potentially be the ER-FB neurons that we describe (Schlegel et al 2024 Nature). We refrain from mentioning this here, as its too speculatory, but we thought the reviewer may be interested in this observation.

> *(4) The details of antibody information are missing in the Key resource table. Instead of citing papers, list the catalogue numbers and identifier for commercially available antibodies, and describe the antigen, and whether they are monoclonal or polyclonal. Are antigens conserved across species?*

We have now added substantial information to Table 2, including research resource identifiers (RRIDs) and antigen descriptions, as well as information about specificity and conservation. In the text itself, in line 757, we already provide publications that have illustrated conservation very extensively.

We believe that with the additional information provided in Table 2, all necessary information is now provided.

> *(5) I did not understand why authors assume that foraging to feed on pollens is a more difficult cognitive task than foraging to feed on nectar. Would it be possible that they are equally demanding tasks, but pollen feeding allows Heliconius to pass more proteins and nucleic acids to their offspring and therefore they can develop larger mushroom bodies?*

This is an excellent point. Our current understanding is that pollen feeding is a cognitively more demanding task, because, a) the density of pollen resources is lower than nectar resources, and b) the competition for pollen is higher (pollen is depleted quickly, and *Heliconius* compete with each other, and other taxa including hummingbirds). There is therefore a benefit to high foraging efficiency, which favours the evolution of learning. This is likely reinforced by the long lives of *Heliconius* which live up to a year, compared to ~4 weeks for most outgroups and the temporal stability of major pollen resources, resulting in a memorised location providing benefit for the long periods of time (Young and Montgomery 2020 Proc B).

We now refer to an additional publication (Young and Montgomery 2020 Proc B) in lines 103-104 for a fuller description of the ecology of pollen feeding, and in the current manuscript simply focus on the impact of mushroom body expansion on the CX.

> ***Reviewer #2 (Public review):***
>
> *Summary:*
>
> *In this study, Farnsworth et al. ask whether the previously established expansion of mushroom bodies in the pollen foraging Heliconius genus of Heliconiini butterflies co-evolved with adaptations in the central complex. Heliconius trap line foraging strategies to acquire pollen as a novel resource require advanced spatial memory mediated by larger mushroom bodies, but the authors show that related navigation circuits in the central complex are highly conserved across the Heliconiini tribe, with a few interesting exceptions. Using general immunohistochemical stains and 3D reconstruction, the authors compared volumes of central complex regions, and unlike the mushroom bodies, there was no evidence of expansion associated with pollen feeding. However, a second dataset of neuromodulator and neuropeptide antibody labeling reveals more subtle differences between pollen and non-pollen foragers and highlights sub-circuits that may mediate species-specific differences in behavior. Specifically, the authors found an expansion of GABAergic ER neurons projecting to the fanshaped body in Heliconius, which may enhance their ability to path-integrate. They also found differences in Allatostatin A immunoreactivity, particularly increased expression in the noduli associated with pollen feeding. These differences warrant closer examination in future studies to determine their functional implication on navigation and foraging behaviors.*

We thank Reviewer 2 for the constructive and thorough review. We believe that addressing these criticisms will have improved this publication.

> *Strengths:*
>
> *The authors leveraged a large morphological data set from the Heliconiini to achieve excellent phylogenetic coverage across the tribe with 41 species represented. Their high-quality histology resolves anatomical details to the level of specific, identifiable tracts and cell body clusters. They revealed differences at a circuit level, which would not be obvious from a volumetric comparison. The discussion of these adaptations in the context of central complex models is useful for generating new hypotheses for future*

> *studies on the function of ER-FB neurons and the role of Allatostatin A modulation in navigation.*
>
> *The conclusions drawn in this paper are measured and supported by rigorous statistics and evidence from micrographs.*
>
> *Weaknesses:*
>
> *The majority of results in this study do not reveal adaptations in the central complex associated with pollen foraging. However, reporting conserved traits is useful and illustrates where developmental or functional constraints may be acting. The implied hypothesis in the introduction is that expansion of mushroom bodies in Heliconius co-evolved with central complex adaptations, so it may be helpful to set up the alternate hypotheses in the beginning.*

Thank you for this relevant comment. We have added to the text in lines 124-128, as follows

“Indeed, these circumstances permit us to test the hypotheses that modifications in the mushroom bodies either occurred in isolation from other integrative centres, or that they occurred in concert with specific changes in centres, such as the central complex. This provides insights into the functional flexibility of two interacting, integrative centres across evolutionary time.”

> *In the main text, the authors describe differences in GABAergic neurons "across several species" but only one Heliconius and one outgroup species seem to be represented in the figures. ER numbers in Figure 7H are only compared for these two species. If this data is available for other species, it would strengthen the paper to add them to the analysis, since this was one of the most intriguing findings in the study. I would want to know if the increased ER number is a trend in Heliconius or specific to H. melpomene.*

This points to imprecise phrasing. We indeed have additional data in other species, but unfortunately not to an extent that would permit quantification of cell numbers, which is why we chose to put these data into the supplement, Fig. S4.

We modified the text to more directly point at the additional data in Fig S4, now reading in lines 362-368

“…, we noticed a pronounced difference in a portion of projections leading into the fan-shaped body and a strong difference in signal inside layer III in our two focal species *H. Melpomene* and *D. iulia*, as well as other representatives of the Heliconiini tribe (Figure S4A-B, Figure 7). To understand how these differences could have occurred, we quantified ER neuron numbers in our focal species, and identified a significant difference, reflecting a 35% increase in Heliconius (t = 4.221, P = 0.004; Figure 7H).”

> ***Recommendations for the authors:***
>
> ***Reviewer #1 (Recommendations for the authors):***
>
> *(1) Add a detailed description about each of the tiff files that were deposited at https://doi.org/10.5281/zenodo.15304965. It was hard for me to relate these raw images with the Figure panels. For instance, "Melp_GAD_26-F_detailed_conc.tif" in the Figure 7 folder seems to be used to make Figure 7L and N, but that information is cryptic.*

We agree with the reviewer. We added further descriptions, and have created a detailed readme file which explains which original file refers to which figure. Together with the efforts for Reviewer 1’s first comment, we hope that this updated version of our repository is easier to understand.

In addition, we made additional changes in image orientation in some of the files supplied, and which were originally incorrect.

> *(2) Add descriptions about the dataset for large-scale volumetric analysis. With the current methods and texts, it is hard to understand what kinds of staining and microscopes were used. I initially thought that they could be micro-CT data.*

We have made two improvements:

We have added an additional readme file to explain the different datasets, and which datasets were used for each figure, to relate them to the original data deposited at *zenodo.org* (see your previous comment).

We have added descriptions in several places in the manuscript file, i.e.

Lines 133-135, now reading "To assess evidence of volumetric changes in the central complex and associated neuropils, we drew data from a large dataset of immunostained brains from 307 individuals of 41 species, …"

Lines 144-149, now reading "We used a combination of phylogenetic comparative analysis across a large dataset of brains immunostained against the structural marker synapsin in 41 species and 307 individuals, and more targeted sampling of species that represent the behavioural and neuroanatomical diversity of Heliconiini for more fine-scale assessments of patterns of divergence in substructures of the CX with various antibodies (Figure 1A-B)."

> *(3) Line 275: Non-expert readers would need an explanation about what the gamma lobe is.*

Agreed and added in line 273

"Some of the ventral projections seemed to directly originate from the γ lobe, a portion of the mushroom body, thus potentially labelling projections of mushroom body output neurons into the fan-shaped body (Figure 5a-c) [12,21]."

> *(4) Figures 4 I-L are missing.*

We modified the figure caption accordingly, and address annotated differences more directly. This section now reads

"G/H: Labelling reveals two distinguishable layers in the fan-shaped body while additional staining elsewhere reveals further detail (arrows in G/H-2/3). Thicker tract conflations indicate the columnar architecture determined through the four columnar neuron bundles (arrowheads in G/H-3). Labelling in the EB reveals two pronounced layers (arrows in G/H-1/2), while obvious columns could not be indicated. PB protocerebral bridge, FB fan-shaped body, EB ellipsoid body. A anterior, P posterior. Scale bars are 50 µm."

> *(5) In the current version of Figure 1B, AOTU is displayed with the mushroom body. The authors can emphasize its relation to the central complex by showing it on the right side of panels together with the central complex.*

Great suggestion. We have done this now. We have kept the AOTU at the scale of the MB, indicated by the different scale bars of the bottom of the figure, as we're showing the CX at a slightly larger scale.

> *(6) Figure 1C: What do the colors of the lines represent?*

We now changed these colours so that they correspond to the colours chosen in Figures 2 and S2 as well as in a previous publication of the lab, added an asterisk next to Heliconius aoede,

and added text to the figure legend:

"Colour indicates focal groups here and elsewhere [29]. The asterisk at the branch of *H. aoede* indicates a secondary loss of pollen feeding."

> *(7) Figures 2A and B: What does the size of the circles represent? I guess that small ones are individuals, and larger ones are species averages. Plots with only species averages would be easier to see. It is difficult to distinguish Heliconius and Heliconnonius aoede in these panels. It would be easier if Heliconius circles were outlined with thin black lines.*

Thanks for this. We wanted to keep both the averages and individual data points in one figure, as to not overcrowd the manuscript with additional figures. We still hope that the changes we made address the confusion sufficiently. We made the following modifications to Figure 2 and S1 and S2:

(1) Added text in the figure legend clarifying what solid and transparent circles indicate ("Solid data points indicate species averages, while opaque circles indicate individual data points.")

(2) Added, as suggested, additional contours, to all *Heliconius* data points, and added corresponding text to the legend ("Black contours indicate Heliconius sp. data points.")

(3) Changed opacity settings of individual data points.

> ***Reviewer #2 (Recommendations for the authors):***
>
> *(1) Line 391 and Methods. It was unclear how the extrapolated microglomeruli numbers were calculated. Please clarify this in the methods.*

Agreed. We substantially modified the text to address this.

Lines 392-396: "We generated high resolution images of the bulb to determine its size (Figure S5 C-F), and 3D segmented seven microglomeruli per individual with which we generated an extrapolated approximation of total microglomeruli number by dividing bulb volume with average microglomerulus volume. This was necessary as most microglomeruli were not discernible from each other (Figure S5 G-H)."

Lines 862-873: "To segment the bulb, we created high resolution images and were particularly careful to only segment the area of the bulb that comprised large synapses/glomeruli, excluding parts of the LEa/IT projection. This was essential, because we relied on extrapolating the total number of microglomeruli from a subset of segmented microglomeruli and the total volume that contained microglomeruli, which means any section containing tracts and not glomerular structures would skew the estimated total number of microglomeruli. Extrapolation was necessary, as not all microglomeruli were visually discernible. We achieved an unskewed bulb volume by leaving out dense pieces of tubulin-positive tract material. We segmented seven microglomeruli per individual from the posterior section of the bulb, where they were most clearly visible, to get the most comparable impression across individuals and species. We then calculated average microglomerulus size and divided this by bulb volume to determine an approximation of microglomeruli number."

> *(2) Line 439. It would be helpful to add that Kaiser et al. studied honeybees.*

Agreed! Now reads in lines 443-444

"Moreover, Kaiser et al. [75] identified Allatostatin A expression in three fan-shaped and two ellipsoid body layers in the honey bee brain, …"

> *(3) Line 492. "outcome" should be "outcomes".*

We believe that this refers to original line 481. Corrected. Thank you.

> *(4) Figure 3B. If there is significance to the colors and triangle directions, please include a key/legend.*

We have added:

“Cell type depictions are examples with localisation inside each neuropil being purely visual (as well as their colour), while triangles indicate approximate output sites.”

We also corrected the following issues that were noted during our revisions:

line 587, wrong reference.

We updated references 37 and 44, which are now respectively

Hodge, E. A. et al. Modality-specific long-term memory enhancement in Heliconius butterflies. Philos Trans R Soc Lond B Biol Sci 380, 20240119 (2025).

Hodge, E. A. et al. Conservation of sensory pathways implies a localised change in the mushroom bodies is associated with cognitive evolution in Heliconius butterflies. Evol qpag005 (2026) doi:10.1093/evolut/qpag005.

Figure S5 had an error in panels C and D, where the pictures in C were actually for *H. Melpomene* in D and the reverse; the other panels were correct. We have corrected this.

In the data submitted on Zenodo: we corrected a few inconsistencies in channel colours and orientation in the .tiff files for Fig 6, 8 and S4.

We added important bulb 3D segmentation files to the repository on Zenodo.

https://doi.org/10.7554/eLife.107589.2.sa0